CHAPTER 1

INTRODUCTION

1.1 Introduction:

According to many researches and experiments, scientists have found that it is possible to create new characteristics of materials by decreasing the dimensions of those materials. They also have found that Nanotechnology plays a very important role in that field. Actually, when the size of the materials dimensions are in the order of (10^{-9} m), there are many factors that affect the materials properties, such as; quantum-sizes effect, surface-to-volume ratio and boundary effect of fundamental structure. For example, continuous reducing the diameter of silicon nanowires from ~7 down to ~1.3 nm leads to gradual increases of the energy band gap of silicon from 1.1 ev up to 3.5 eV. In fact, this technology attracts intensive interests and attentions of many physicists and chemists. [1].

Nanotechnology, as it is defined in language dictionary, is a science of making or working with things that are so small that they can only be seen using a powerful electron microscope. Nanotechnology has very important applications in many fields including nano-physics; nano-chemistry; nanomaterials science; nano-biology; nano-electronics; nano-machining; and nano-mechanics. Nanomaterials are defined with at least one dimension between 1 and 100 nm. Nanomaterials can be classified into three groups according to the number of dimensions; zero-dimensional materials, one-

dimensional materials and two-dimensional material. Table (1.1) will explain the characteristics of each type of Nanomaterials.

Nano materials classification	zero-dimensional materials	one-dimensional materials	two-dimensional materials
Number of dimensions which have Nanoscale size	materials with nanoscale size in all three dimensions	materials with nanoscale size in two dimensions	materials with nanoscale size in only one dimension
Examples	nanoparticles & nanoclusters	Nanowires, nanotubes, nanocables & nanobelts	Super thin films, multiple layer films & supper lattices

Table 1.1 the classification of nano materials dimensions.

Nanowires, which are considered as one-dimensional material, can be classified into two kinds: metallic nanowires and magnetic nanowires. Non-magnetic materials such as Pb and Au can be used to produce metallic nanowires while magnetic materials such as Fe and Ni are used to synthesis magnetic nanowires. [1] and [2].

Thermoluminescence dosimeters are one of the famous radiation detectors. They are sorted as a kind of detectors because they have been used in the radiation field to determine the amount of the radiation stored after exposed. For example, TLD (the short form of Thermoluminescence dosimeter) reader is used to measure the amount of radiation stored as Thermoluminescence emission for each trapped electron. There are many materials which are used as Thermoluminescence dosimeter, such as, lithium fluoride (LiF) and calcium fluoride (CaF_2) dosimeters. ZnS could also be considered as Thermoluminescence dosimeter because it has been found that ZnS crystals have high photoluminescence and thermoluminescence properties above room temperature [23]. ZnS crystals are widely used in opto-electronic devices because of their photoluminescence properties.

In this experiment the Zns particles will be used as Thermoluminescence dosimeter and its properties will be studied. ZnS crystals produced using vacuum evaporation or

chemical techniques have thermoluminescence property emit light that can be best described by a "glow curve", which may present several glow peaks during a heating process.

This study will be divided into two parts. The first part is to synthesis ZnS nanoparticles and the second part is for tasting TL glow carves for the resultant ZnS nanoparticles. In this research, ZnS particles will be synthesized by method of thermal evaporation of Zn powder and S powder onto silicon substrates. The second method which is used to produce ZnS naon particles is by chemical precipitation method. ZnS:Mn nanoparticles will be synthesized by using solutions of three chemical compounds which are Zinc sulfate, Sodium sulfide and Manganese sulfate. The morphologies of resultant ZnS nanoparticles will be examined by FESEM, XRD and EDX. Finally the TL properties of ZnS nanoparticles and normal ZnS commercial powder will be studied. Then comparison between the results will be done. The ZnS nanoparticles will be used as dosimeter .

1.2 Objectives of the research:

1- Synthesis ZnS nanoparticles by method of thermal evaporation of Zn and S powders.
2- Synthesis ZnS and ZnS: Mn nanoparticles by method of chemical precipitation.
3- Comparing the TL of ZnS commercial powder with TL of ZnS nanoparticles.
4- Using ZnS nanoparticles as a TL dosimeter.

1.3 Outline of the dissertation

The first chapter of this dissertation gives a general view of nanoparticles also the chapter includes the objective of the research. Chapter two gives a description of Zinc Sulfide which includes crystal structures such as zincblende structure and Wutrzite structure, Physical Properties of Sulfur and Zinc and Bonding in II-VI compounds. Various techniques for synthesizing ZnS nanowires and prior approaches used to

fabricate ZnS nanowires are also discussed. Finally characterization techniques such as transmission electron microscopy (TEM), scanning electron microscopy (SEM), Energy Dispersive x- ray Spectroscopy (EDS) and x- ray diffraction are discussed in this chapter.

Chapter three will include the methods which were used to synthesize ZnS nano particles using thermal evaporation and chemical precipitation techniques. The construction of the apparatus and preparation steps of ZnS nano particles will be explained. Chapter four shows the characterization of synthesized ZnS nano particles using high resolution scanning electron microscopy FESEM, XRD and EDX. The results and the discussion of ZnS and ZnS: Mn nano particles Thermoluminescence properties are presented in chapter five. Finally concluded the experiment results and gives some suggestions to enhance the Thermoluminescence properties of ZnS nano particles and to use this suggestions for further future studies.

CHAPTER 2

LITERATURE REVIEW

2.1 Introduction:

The productions of semiconductors were basically produced by a type of materials in the periodic table. These materials were called II-VI compound materials. They were known as "crystal phosphors" and were used as cathode ray tube screen materials in the third decade of this century. In the last fifties, II-VI compound materials had a boom in colored television tubes and their present production output in the nearly comparable with Si. Of course their outstanding merits are not in their semi-conducting properties which have to compete with Si but nevertheless they are semiconductors-adequately understandable and describable by the concepts of semiconductor physics [3].

Compounds which are formed by metals, such as, Zn, Cd and Hg of column II of the periodic table and the chalcogens O, S, Se and Te of column VI have wide energy gapes between the valence and conduction bands which give them a great advantage. This wide energy gap gives those materials higher optical transmission probabilities for absorption and luminescence so it was used in the early days for luminescence in the visible region. These compounds have high ionicity which makes them good candidates for having high electro-optical coupling and electromechanical coupling constants. In the last 50 years, physicists are interested in studying the physical properties of the II-VI

compounds which has stimulated considerable research into methods for growing signal crystals as well as thin films of these materials [3, 5].

ZnS, which is among II-VI compounds, is a good material to study and use in the preparation and characterization for both academic research and industrial purposes because Zns is a very promising candidate for such technological application, especially for light emitting diodes and hetero junction devices [3].

2.2 description of Zinc Sulfide crystal structures

Zns has two forms zinc blende_and wurtzite which are found in the natural. Wutrzite form of ZnS is stable at high temperature and it has been found that the inversion temperature of 1020°C and 1150°C are suitable to change the hexagonal to cubic [5]. In additions it is reported that there is some variation in the lattice constants of both cubic and hexagonal modifications. This variation could happen because of impurities and imperfections in the crystal structure. The replacement of S by O is common impurity. ZnS has a wide band gap of 3.72 eV (333.6 nm) for the cubic phase and 3.77eV (329.2 nm) for the hexagonal-wurtzite phase. [2].

2.2.1 Zincblende structure

All of the II-VI compounds form crystals with the zincblende (fig. 2.1). In the unit cell, there are four ZnS and all atoms are in special positions with 4S and 4Zn. If both kinds of atoms were the same, the arrangement would be the same as in diamond. That means that four atoms from one kind are surrounding one atom from another kind. For example, each (Zn) is surrounding with four nearest neighbors of (S), and vice versa, at a distance of $1/4\sqrt{3a}$ at the corners of a regular tetrahedron, where (a) is the cubic lattice parameter. There are twelve next-nearest neighbors of atoms of the same kind at the distance $2\sqrt{2a}$. Six of these are distributed at the corners of a hexagon in the same

plane as the original atom; the remaining six forms a trigonal antiprism with the three above and three below the plane of the hexagon. [5].

2.2.2 Wutrzite structure

The II-VI compounds can crystallize to form wurtzite (fig. 2.2). There are two molecules in the hexagonal unit cell with two Zn and two S. At the corners of tetrahedron there are approximately four S atoms surrounding Zn atoms. There are twelve next-nearest neighbors; six at the corners of a hexagon in the same plan as the original atom. The remaining six are at the corners of a trigonal prism. [5].

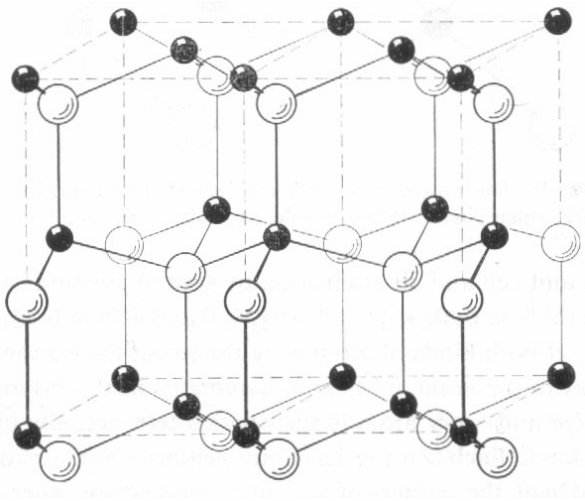

Figure. 2.1. Zincblende. The arrangement of metal atoms (small filled circles) and non-metal atoms (large-open circles) in Zincblende, the cubic form of Zns. [3] .

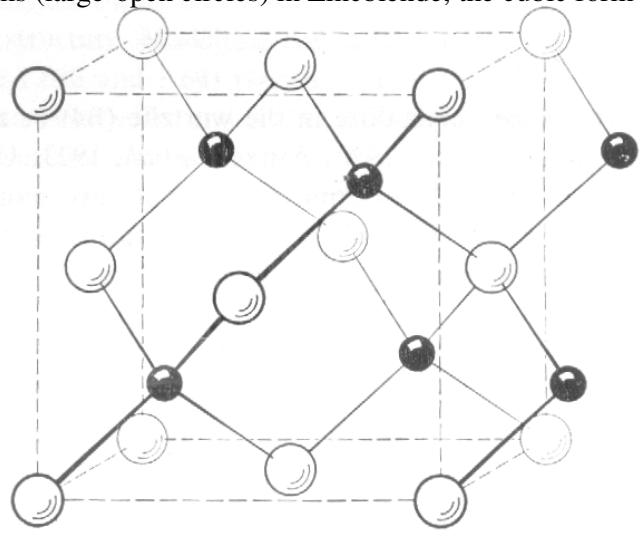

Figure. 2.2. Wurtzite. The arrangement of metal atoms (small filled circles) and non-metal atoms (large-open circles) in wurtzite, the hexagonal form of Zns. [3] .

2.3 Bonding in II-VI compounds

The electromagnetic interaction between the positively charged nuclei and negatively charged electrons of the constituent atoms create the forces that bind a solid. Actually, it has been found that the electronic structure of the different atomic states plays an important role in the interactions but still it is not yet possible to make or formulate a theory for the binding in all solids.

In general, the binding forces depend on the positions of the atoms in the periodic table, the semiempirical theory of chemical bonding and the structure. Actually, Chemical bonds are classified into three general types: ionic bonds, covalent bonds and metallic bonds. The bonds in the most II-VI compounds are adequately described by any of these extreme types, but have characteristics intermediate to those usually associated with the terms ionic and covalent.

The following chart will illustrate the three types of the chemical bonds.

Table 2.1 the types of bonds and there position in the periodic table

TYPES OF THE BONDS	POSITION IN THE PERIODIC TABLE
Ionic Bonds	Between atoms that are located in the extreme left-and right hand portions of the periodic table.
Covalent Bonds	Between atoms that are located near the centre of the periodic table.
Metallic Bonds	Between the elements displaying characteristic high thermal and electrical conductivity that are located principally in the lower left region of the periodic table.

When an electron from metallic element transfers to nonmetallic element, ions are formed. Ionic bond is produced as a result of an attraction due to Columbic force between the excess positive and negative charges. In ZnS, for example, transfer of

$4s^2$ electrons from Zn to the 3p orbital of S forms ions with stable closed shell configurations: $Zn^{+2}(3s^2 3p^6 3d^{10})$ and $S^{-2}(3s^2 3p^6)$. Although the II-VI compounds were originally classified as ionic solids, but according to calculations of the crystal energies of the sulfides and selenides. It was concluded that the binding is not necessarily completely ionic. The interatomic separations that are found in II-VI crystals with the zincblende or wurtzite structure can not be explained only by pure ionic model. The study shows that the calculated distances between the II and VI atoms is larger than those observed. This is due to covalence effects, the covalent shortening increases with increasing atomic number. The distribution of electrons can be obtained from the X-ray diffraction; studies of this kind have been made on ZnS and obtained projections of the electron density in ZnS planes which concluded that the bonding was a mixture of ionic and covalent. [5].

2.4 Sulfur

There are many elements which are found in the free state in the nature. Sulfur is one of them which is known and used by our earlier ancestors. Sulfur is a very important element. Students and chemists recognize the importance of sulfur and their compounds in chemical industry and environment. More than 100 million tons are produced per annum. This element is very important not only for heterogeneous catalysis and for application of solid state electrochemistry with respect to technological aspects but also for the evolution of our geosphere.

2.4.1 Physical and Chemical Properties of Sulfur

Sulfur is a much known element which has many characteristics that make it a special and an important element which is used in many fields in physics and chemistry. Sulfur is a bright yellow nonmetal. Pure sulfur has no taste or smell and it is not harmful to people while its compounds smell very strongly and some of them are harmful to people (poisonous). Sulfur is used a lot in the inorganic industry.

Oxygen O, sulphur S, selenium Se and tellurium Te, that occupy column VIA of the periodic table. All are nonmetals, and their oxides form acidic solutions in water. The atomic number of sulphur is 16, its atomic weight 32.07 amu, and its electron configuration is $(1s^2 2s^2 2p^6 3s^2 3p^4)$, with six valence electrons outside a neon core. The first ionization potential of the atom is 10.357 V, the second is 23.405 V, so the atom holds its electrons quite strongly. Further more, it is available in the nature to the amount of 0.052%. It has been mentioned that the structure of S affects on its existence. If a neutral atom gains two electrons, it completes the stable argonic structure. The sulphur ion S^{--} is stable in aqueous solution, where the polar water reduces the energy penalty of the charge. Two sulphur atoms can make a "coordinate covalent" single bond, and this S_2 molecule is found in the vapor at high temperatures. Sulphur does not form $S_2$with a double bond, as oxygen does. If two electrons are added to this molecule, the result is the disulphide ion, S_2^{--}, which is also stable in aqueous solution. [8].

2.4.2 Forms of sulfur

Sulfur has different solid forms in the nature. These forms are called auotropes. These forms differ from each other in the physical properties. There are eight sulfur atoms bonded together as a ring-shaped molecular in the two most important allotropes. .The crystal structure of orthorhombic sulfur (fig. 2.3), the cell parameters are a: 1043.7 pm, b: 1284.5 pm, c: 2436.9 pm, $\alpha: 90^\circ$, $\beta: 90^\circ$, $\gamma: 90^\circ$

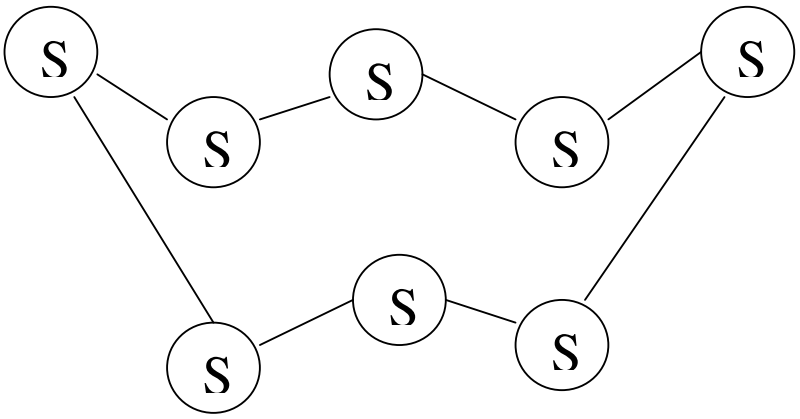

Figure. 2.3. Covalent Sulphur molecular solid at room temperature with the formula S_8

As it is mentioned about that there are many solid forms of sulfur. For example, Alpha , Beta, Plastic, Roll, flowers and Molten. Each one has different physical properties. For example, Alpha sulfur forms a bar crystals in an arrangement called orthorhombic system. It is stable below 96 C. On one hand, Beta sulfur forms bright yellow chisel-like crystals in an arrangement called the monoclinic system. This type of sulfur is stable in $96^{\circ}c$ to the melting point $118.9^{\circ}c$. The third form of sulfur is called plastic sulfur. Pouring molten sulfur into cold water will produce plastic sulfur which is soft and rubbery. It is made of long chains of sulfur atoms. Other forms such as roll and flowers sulfur has a mixture of different sulfur allotropes.

The temperature of the sulfur may determine the physical characteristics of some sulfur form such as Molter sulfur. For example sulfur becomes a runny amber liquid when it is above its melting point. When more heat is applied the molar sulfur becomes thicken and darker. This is because the ring-shaped molecules break a pant and form long jumbled chains. When the temperature is near the boiling point, the sulfur becomes a black liquid because the chains begin to fall a part. In conclusion, temperature has a main hand in producing different sulfur forms because it plays in its structure which determines different physical properties. [9].

2.5 Zinc

Zinc was known thousands of years a go. Egyptians used zinc in the form of bronze as long as 2200Bc while Romans used brass-another form of zinc- around 200Bc.

Brass most probably came into usage when Smith Sonita was unknowingly smelted with copper to yield a new alloy, more yellow and more attractive than bronze. In that time, zinc was not considered as metal. It was discovered as metal in 1520 AD. During the Medieval period ,zinc mining was developed in Spain, Cornwall, Sweden, Saxony, and some areas of eastern Europe but mining was still unorganized. It was first organized in U.S.A in 1720 than in Europe in 1790. Because of the importance of zinc, zinc production raises to 704 million tones in 1992. [8].

2.5.1 Physical and chemical Properties of Zinc

Zinc is available in the nature. It is an abundant as rubidium, at the same time, it is more abundant than copper. Zinc is located in the 12^{th} column of the periodic table. As other metal, zinc has its physical and chemical properties. It is a bluish-grey metal. In air zinc is just like a sheet of aluminum but it is heavier than aluminum and it does not bend easily. Its atomic number is 30, atomic weight 65.38. Its natural occurring isotopes are 64 (49%), 66 (28%), 67 (4%), 68 (19%) and 70 (0.6%). Its density is 7.14 g/cc, electrical resistively 6.16 μΩ-cm, heat capacity 0.0925 cal/g-K, and heat conductivity 0.268 cal/cm-s-K. Zinc melts at 419.5°C and boils at 907°C. Its crystal form is hexagonal close packed, with a = 0.266 nm, c = 0.494 nm. The ionic radius of Zn^{++} is 0.074 nm. The ionization potentials of zinc are 9.36V and 17.89V. The electron configuration of zinc is $1s^2 2s^2 2p^6 3s^2 3p^6 3d^{10} 4s^2$. The atom shows a valence +2 in their compounds. Zinc is covered by a productive transparent layer of hydrogen gas or (polarization), as a result of this hydrogen layer pure sulfur does not react with water or dilute acids.

Arsenical zinc is used for making hydrogen in the chemical laboratory. The reduction potential of zinc is -0.76V, and of cadmium, -0.40V, so both are relatively reactive. [8].

The crystal structure of zinc is hexagonal close-packed (fig. 2.4), the cell parameters are a: 226.49 pm, b: 266.49 pm, c: 494.68 pm, α: 90°, β: 90°, γ: 120°

.

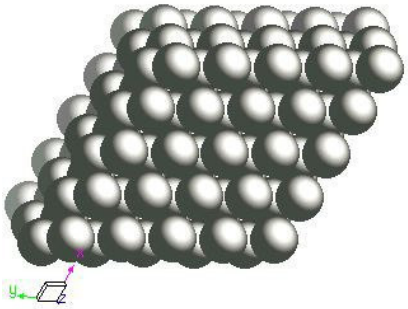

Figure. 2.4. Structure of Zinc crystal.

2.6 Nanostructures Syntheses and fabrication techniques

Two categories of syntheses and fabrication techniques are generally used. One is called "bottom-up" techniques and the other one called "top-down" techniques. The "bottom-up" can be approached by using the chemical properties of single atoms to automatically arrange themselves into some useful conformation such as dots or wires. [2]. It all begins from atoms and molecules that get rearranged and assembled to larger nanostructures. Thermal decomposition, laser assisted vapor-liquid-solid and thermal evaporation are some examples of "bottom-up" synthesis methods.

"top-down" techniques which are fabricate nanoscale objects out of bulk materials by cutting, milling, and shaping those materials into the desired shape, order and dimension by using micro fabrication method such as wet etching, dry etching and reactive ion etching. It begins from a bulk piece of material, which is then gradually or step-by-step

removed to form objects in the nanometer-size regime. Nanowires can be synthesis by two methods gas-phase synthesis and solution-based synthesis.

A lot of techniques have been used in the synthesis of one – dimensional nanostructure materials. This technique can be summarized in fig. 2.5.

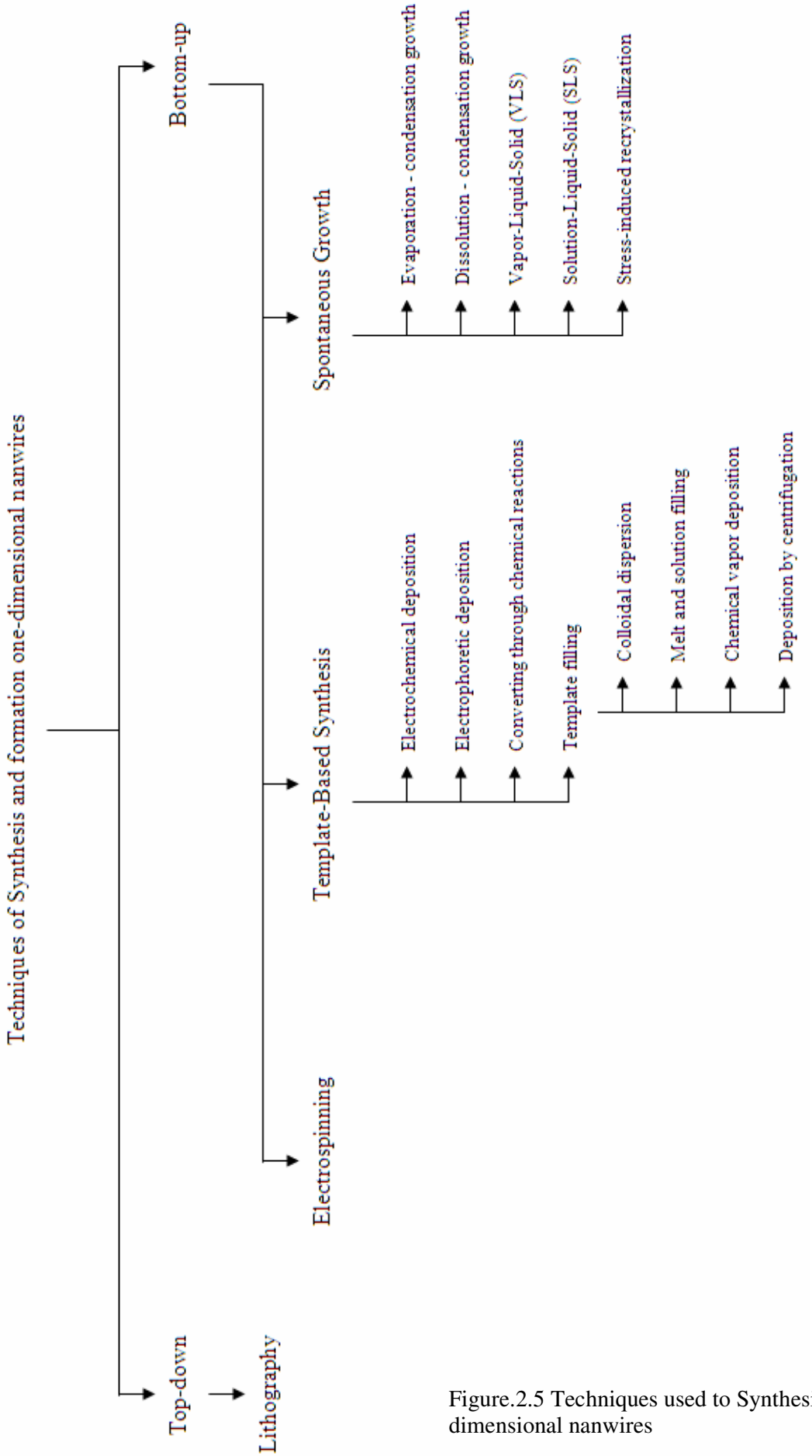

Figure.2.5 Techniques used to Synthesis one-dimensional nanwires

2.7 Gas-Phase Synthesis

2.7.1 Vapor-liquid-solid (VLS)

VLS was found in the early 1960s. This mechanism is very important so it has success in the growth of semiconductor nanowire. Actually VLS is the mechanism which is mostly used in producing and creating nanowire. This method has been used to fabricating nanowire with assistance to some facilities. To use this method some equipments are needed. A horizontal ceramic tube furnace is required which is attached to constant gas flow (such as Ar gas or N_2 gas). Au particles are used as a catalyst and it is deposited on Si wafer and they are exposed to heat which reach a temperature of (about $363^{\circ}C$). The substrate is annealed. As a result of that Au react with Si to form Au-Si alloy droplets which is the base of nanowire growth. (Fig 2.6).and (Fig 2.7).

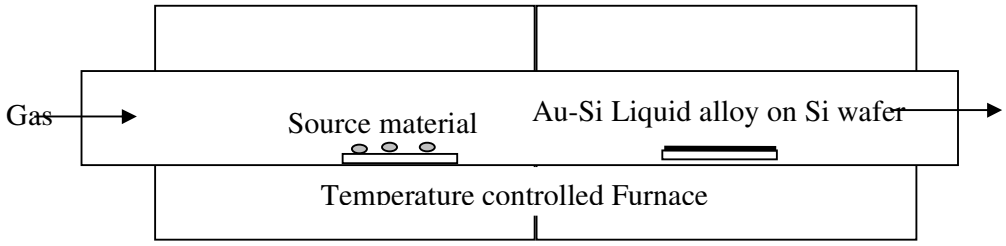

Figure. 2.6 Schematic of tube furnace for vapor– liquid-solid growth.

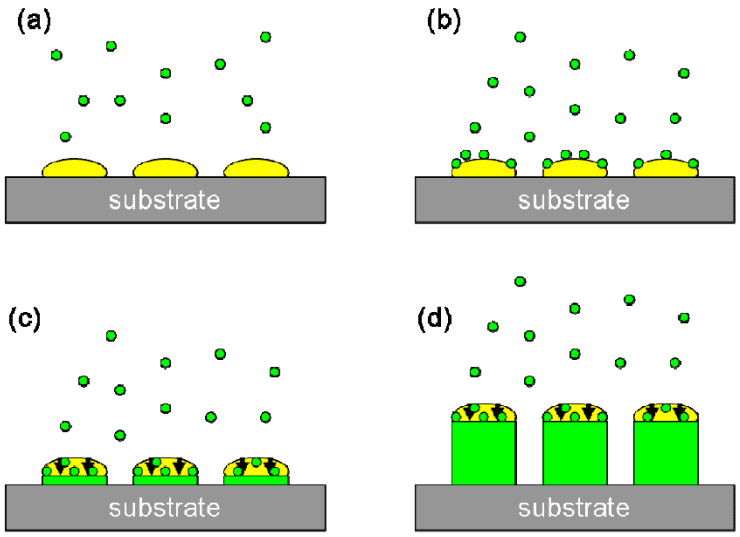

Figure. 2.7 The schematic diagram of traditional adsorption-induced VLS model : (a) mass transport of vapor species, (b) intermediate reaction at the vapor–liquid interface, (c) penetration of the product to the melt and subsequent diffusion to the liquid–solid interface, and (d) incorporation into the solid at the liquid–solid interface and growth [11].

2.7.1.1 Physical vapor deposition (PVD)

It is the short form of physical vapor deposition. The thermal evaporation of sources that is a bulk version of the desired nanomaterial, produces the vapor species. Most of these materials are commercially formed in powder form. This material could react with a gas to be cooled and redeposit on a substrate. The small molecules can be relased from its bulk materials by many methods. Those methods will stimulate and remove the molecules by thermal processes or by kinetic energy deposition. The thermal excitation can be obtained from thermal evaporation (electron beam heating or flame synthesis), or by laser ablation (when a short nanosecond pulse from a laser is focused onto the surface of a bulk target), sputtering is a method which use kinetic energy to release molecules from its bulk by bombardment with atoms or ions. [14]. The main benefit of PVD is that it can provide for easy control over the chemistry of the synthesized material, with relatively little control of the system parameters. [13].

2.7.1.2 Chemical vapor deposition (CVD)

CVD is the second type of VLS. It is the short form of chemical vapor deposition. A chemist believes that chemical reaction plays very important role in creating something new. According to CUD, a chemical reaction creates the vapor species. For examples, when chemical reaction happens between Zn and H_2S flow gas / ZnS vapor species will be produced. Chemists have found that it is important in CVD to control the atmosphere as it is difficult to achieve the correct setup.

2.7.1.3 Laser-assisted catalytic growth

In this method a heated flow tube is used, the target is placed in the tube with constent flow of carrier gas such as (Ar) or (H_2). The target consists of mixture of catalyst metal and nanowire materials. The laser beam is focused in the target so, the evaporation is obtained by laser beam. Then this vapor is carried by gas and solidifies into substrate (fig. 2.8). Laser ablation has advantage compared to other synthesis techniques because laser can be used to generate nanometer-size for many material.[12]. In some cases the laser beam provides an enough kinetic energy; which is deposited to nanomaterial molecules. The molecules can move and solidifies by themselves. So, in this method it is some times no need to use carrier gas.

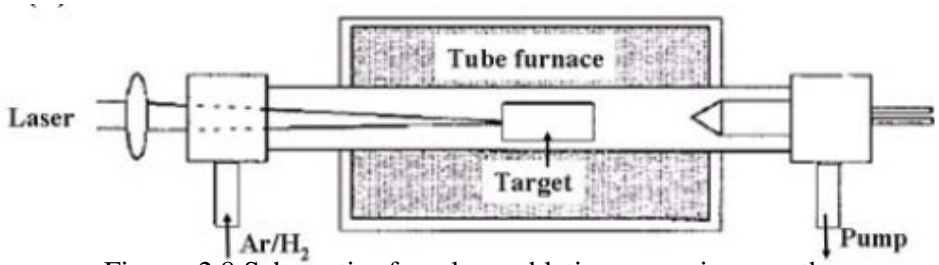

Figure. 2.8 Schematics for a laser ablation nanowire growth apparatus.[12]

2.7.2 Vapor-solid (VS) process

This method can be used to syethises nanowires without using a metal catalyst as a liquid droplets. It is an evaporation condensation growth, the sours material is heated near its melting point then carrier gas will transport the vapor particles and condensed onto a substrate the deposition happen at cooler temperature. Vapor-solid mechanism and the Vapor-liquid-solid are nearly the same. The deference is that in (VS) the one component of the gaseous atoms might play the role of the catalyst itself. (fig. 2.9). Dissolution – condensation process differs from evaporation – condensation in growth media. In the Dissolution – condensation process, the desire nanowire materials are first dissolve into a solvent or solution, and then diffuse through the solvent or solution and deposit onto the surface resulting in the growth of nanowires.

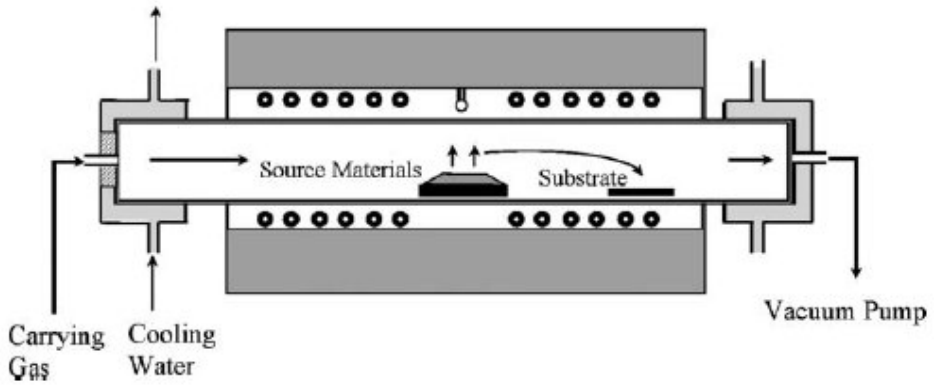

Figure. 2.9 Schematic of tube furnace for vapor-solid growth.

2.7.3 Oxide-Assisted Growth (OAG)

Some materials can be developed into nanowires from their oxide decomposition. For example it was found that no need to use metal catalyst for producing Si nanowaires, Sio_2 has been found to be an effective catalyst which makes Si nanowires to growth. In this method the target is a mixture of Si and Sio_2 powders and no metal catalyst is needed. Wang et al used this method to produce Si nanowire by laser ablation of the target[15]. By this method a very uniform Si nanowires was formed with

diameter of 20nm and 100μm in length. The mechanism of the Oxide-Assisted Growth can be described by the following reactions.

$$Si\ (solid) + SiO_2\ (solid) \xrightarrow{high\ temperature} 2SiO\ (gas)$$

$$2SiO\ (gas) \xrightarrow{low\ temperature} Si\ (solid) + SiO_2\ (solid)$$

$$SixO(gas) \xrightarrow{low\ temperature} Si_{x-1}(solid) + SiO\ (solid)\ (x > 1)$$

By laser ablation, Si reacts with SiO_2 to form SiO or SixO (x>1) vapor phase. This vapor phase is the key factor for the nucleation and growth of Si nanowires because it deposits on the substrate and decomposes into nanoparticles at a relatively low temperature of 900-1000°C.[12]. The nanowires have a thin oxide layer covering a crystalline Si core. (fig. 2.10).

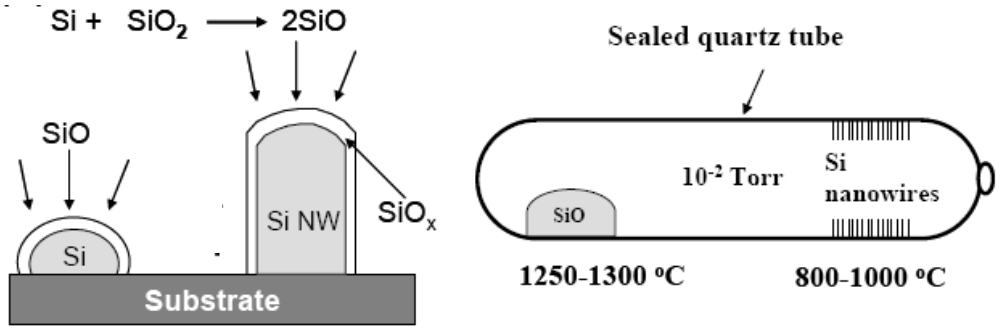

Figure. 2.10 Schematics description of the oxide assisted Si nanowire growth process and Experimental set-up for oxide assisted method.[12]

2.8 Solution-Based Synthesis

2.8.1 Electrochemical deposition method

Electrochemical deposition is one method which is used in Template-Based synthesis technique. There are many kinds of template but the most commonly used is anodized alumina membrane, Alumina membranes with unform and parallel pores structure are made by anodic oxidation of aluminum sheet in solution of sulfuric, oxalic

or phosphoric acids [16]. This pores are arranged in a regular hexagonal array with a density of $10^{11}\ pores/cm^2$. The template with pores of diameters ranging from 10 to 200 nm is placed in a deposition solution and is connected to the cathode. Pores can be filled with desired nanowire material by deposition of solid material on an electrode. That can be done when anode is placed in the deposition solution parallel to the cathode. When the electrical current is applied to the circuit, the cations reduce at the cathode so, the growth of nanowires occurs inside the pores of the template.

2.8.2 Solution-Liquid-Solid (SLS) Method

A low temperature solution-liquid-solid (SLS) method for the synthesis of highly crystal nanowires was first introduced by Buhro and coworkers [15]. This method is the same as VLS growth method but it can operate at low temperature and use solution phase reactions. SLS method is used to produce crystalline nanowires of III-V semiconductors. A metal with low melting point such as (In,Sn,Bi) was used as a catalyst and the desired material was generated through the decomposition of organometallic precursors. Growth of (Inp) can be used as example, The precursor used is typically an organometallic compounds as $In(t\text{-}Bu)_3$ and PH_3 which are dissolved into a hydrocarbon solvent. In the solution the precursors reacts to form (In) and (P) compounds for the growth with the following reaction:

$$In(t-Bu)_3 + PH_3 \rightarrow InP + 3(t-Bu)H$$

Indium metal functions as the catalyst for the growth of (InP) nanowires. In melts and forms liquid droplets. Both (P) and (In) dissolve into the droplets and precipitate to form the (InP) nanowires. (fig. 2.11).

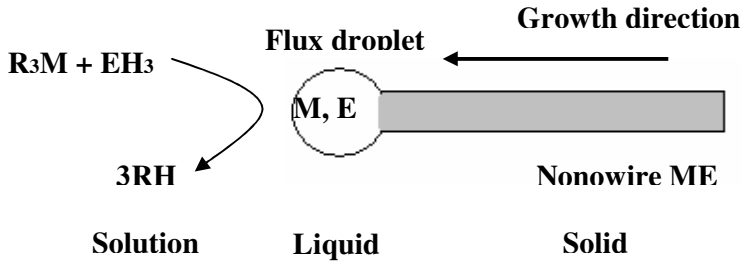

Figure. 2.11 Schematics showing the growth of nanowire through the solution-liquid-solid mechanism.

2.9 Prior approaches used to fabricate ZnS nanowires

In 2003 X.M Meng reported the synthesis of ZnS nanowires by using the VLS mechanism[17]. High-purity ZnS powder were put in an alumina boat which was located at the center of the quartz tube. A silicon wafer substrate covered with 3nm Au film was placed in the tube at a distance of about 30cm from the center of the alumina boat. The tube was evacuated to 2×10^{-2} Torr and then a mixture of Argon gas and 5% of hydrogen gas was kept flowing through the tube. The pressure inside the tube was kept to be 300 Torr and the flow rate was 50 sccm, the furnace was then heated at a rate of 25 ° C/min to 800 ° C and held at that temperature for 30 min. the furnace temperature was then raised to 1100 ° C for 3 h and then the furnace was kept to cool to room temperature. The deposited products were characterized with scanning electron microscopy(SEM), X-ray diffraction(XRD) and transmission electron microscopy (TEM). The SEM image of the deposition showed that the substrate was coverd uniformly with a high density of ZnS nanowires with diameters in the range of 10-20 nm and lengths of several micrometers.

Heesung Moon in 2006 [18], presented a synthetic method of fabricating zinc sulfide nanowire by chemical vapor transport and condensation. That was done by the reaction of zinc oxide and iron sulfide powders on a silicon substrate coated with 50μm

gold film . ZnS is formed when ZnO reacts with FeS under a temperature of (1200°C to 1380°C) according to the reaction formula $ZnO(powder) + FeS(powder) \rightarrow ZnS + Fe_3O_{4-x}$ Equal amounts of pure ZnO and FeS powders were mixed in an alumina boat, which was inserted to a quartz tube into a horizontal tube furnace. The furnace temperature was increased to 900°C to 950°C in constant Ar flow. ZnS nanowires were grown on gold coated silicon substrates through a simple chemical vapor transport-condensation based on the vapor-liquid-solid(VLS) mechanism. In the previous reaction FeS has an advantage in prevent oxidation of the produced ZnS nanowires because at high temperatures the iron atoms decomposed form FeS and react with oxygen atoms. As a result of that Fe_3O_{4-x} were produced in the alumina boat. The sample was cooled down to room temperature, it was found that the substrate surface was covered by white ZnS nanowires. The produced ZnS nanowires was characterized using scanning electron microscopy, transmission electron microscopy and dispersive X-ray spectroscopy (EDXS). The image from (SEM) showed that the ZnS nanowires had a diameters ranging from 10 to 30 nm and lengths up to several hundred micrometers.

ZnS nanowires were successfully synthesised by Z. Xianghui in 2005 [19] in large quantities via simple thermal physical evaporation without using any metallic catalyst. A bout 1 gram of ZnS powder was loaded in a quartz boat which was then placed in the center of tube furnace and silicon wafer was located at about 10cm from the boat. Argon gas was used as a carrier with constant flow of 95sccm also hydrogen gas was used with flow rate of 7sccm, the furnace temperature was raised to $100^\circ C$ for 30 minute with 0.05 Mpa furnace pressure. After colling down a white layer was deposited on Si wafer.

A synthesis of ZnS nanowires on an Anodic Aluminum Oxide (AAO) template coated with Au was reported by H. Xintang and T. Ming in 2006.[20]. Pure ZnS powder was placed in the middle of a quartz tube and the substrate was placed next to the senter along the down stream of flow of Ar mixed with 5% of H_2 at rate 50 and 16 sccm. The furnace was heated to $800^{\circ}C$ and after 30 min the temperature was raised to $1100^{\circ}C$ and fixed at that degree for 150 min. After that the quartz tube was removed from the furnace and it was cooled down to $400^{\circ}C$ under the flow of Ar gas. White product was found on the template and single crystal ZnS nanowires were obtained on the whole area of the AAO template. The products were charcterized and analyzed by (SEM), (EDS) and (TEM). The produced nanowires had a diameter of 80nm with length of several tens micrometers.

Thiourea which is an organic compound of carbon, nitrogen, sulfur and hydrogen, with the formula CSN_2H_4 or $(NH_2)_2CS$ can be used as a sulfur source for producing ZnS nanowires when the thiourea is mixed with zinc acetate . The mixture is dissolved in a pure water and ethylenendiamine to produce an aqueous solution of EN, or pure a solvent of ethylenediamine. This method was reported in 2006 by G.H. YUE [21] to synthesis ZnS nanowire. The solution was placed in a Teflon cup then the temperature was raised to $180^{\circ}C$ for several hours. After cooling down, a white product was obtained through filtering and washing with alcohol and distilled water to remove impurities. In this experiment the concentration of zinc acetate $[Zn(CH_3COO)_2.2H_2O]$ was 0.40 M and thiourea 0.80 M. The products were characterized by X-ray diffraction (XRD), scanning electron microscopy (SEM) and high resolution transmission electron microscopy (HRTEM).

2.10 Thermoluminescence

The emission of light from a material following the initial absorption of energy from an external source for example ultra-violet or high energy radiation is called Luminescence. The emission can be fluorescence or phosphorescence. That is according to the characteristic lifetime τ between absorption of the excitation energy and emission of the luminescence. If $\tau \leq 10^{-8} s$, the process will be fluorescence. On the other hand if $\tau \leq$ few seconds, the process will be phosphorescence. The delay of time between the two processes can be explained by using a ground state energy level (g) and an excited state level (e), as shown in (figure 2.12). Fluorescence is the emission of light which follows the excitation of an electron from (g) to (e) and it is subsequent return to level (g). lifetime in the exited state may be very short because the exited electron is transmitted immediately to ground state. On the other hand in phosphorescence, the residence of exited electrons in the metastable level (m) delay the return of electron to ground state so, the lifetime is longer in this case. As the temperature increases the probability for the thermal excitation from the trap is increase exponentially. [5]

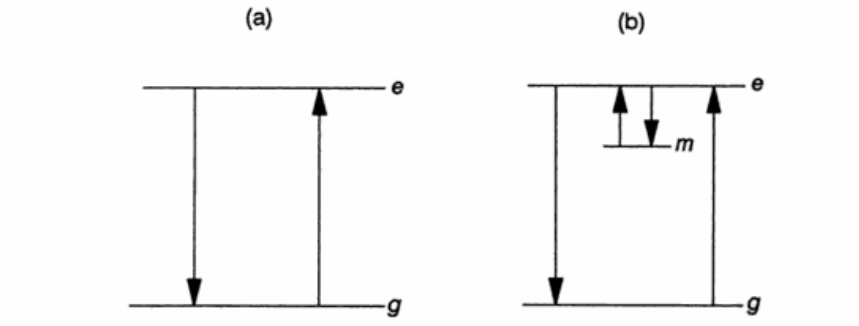

Figure (2.12). (a) Excited e and ground stat (g)energy levels showing absorption and emission for the process of fluorescence. (b) metastable level (m) giving rise to a delay between excitation and emission during the process of phosphorescence.

The thermoluminescence phenomenon had been noted as early as 1663 when it was reported that a diamond was observed to emit light when warmed in the dark. Thermoluminescence is the phenomenon by which certain crystals are able to store

energy transmitted to them by radiation and then emit this energy in the form of visible light when heated. In 1953, it was proposed that thermoluminescence can be used as a radiation detector. To be useful for dosimeter, a TL material must have a relatively strong light output and be able to retain trapped electrons for resonable periods of time at temperatures encounted in the environment. Thermoluminescence detectors often use crystals that are purposely flawed by adding a small concentration of impurity as an activator. Some thermoluminsence detectors do not require an activator but rely instead upon inherent impurities and defects in the natural crystal.

2.10.1 General model of thermoluminescence

As shown in (figure 2.13), thermoluminescence process can be explain by a simple model. The outer atomic electronic energy levels in an inorganic perfect crystal lattice are broadened into a series of continuous allowed energy bands separated by forbidden energy regions. The valence band is the highest filled band which is separated by several electron volts from lowest unfilled band which is called the conduction band. Electrons are excited out of the valence band into the conduction band when a crystal is exposed to radiation. That will leave a vacancy in the valence band called a hole. The electron and hole are free to wander independently throughout their respective bands. Within the forbidden region between the valence and conduction bands there are discrete local energy levels as a result of the presence of lattice defects or impurities. These discrete energy levels trap electrons which on subsequent heating and recombination causes thermoluminescence. The temperature required to release the electron and produce the thermoluminescence are determined by the energy gap between the valence and conduction bands. If the temperature of the crystal is increased, the probability of releasing an electron from trap is increased, so the emitted light will be weak at low temperatures, pass through one or more maxima at higher temperatures, and decrease again to zero as no more electron filled traps remain.

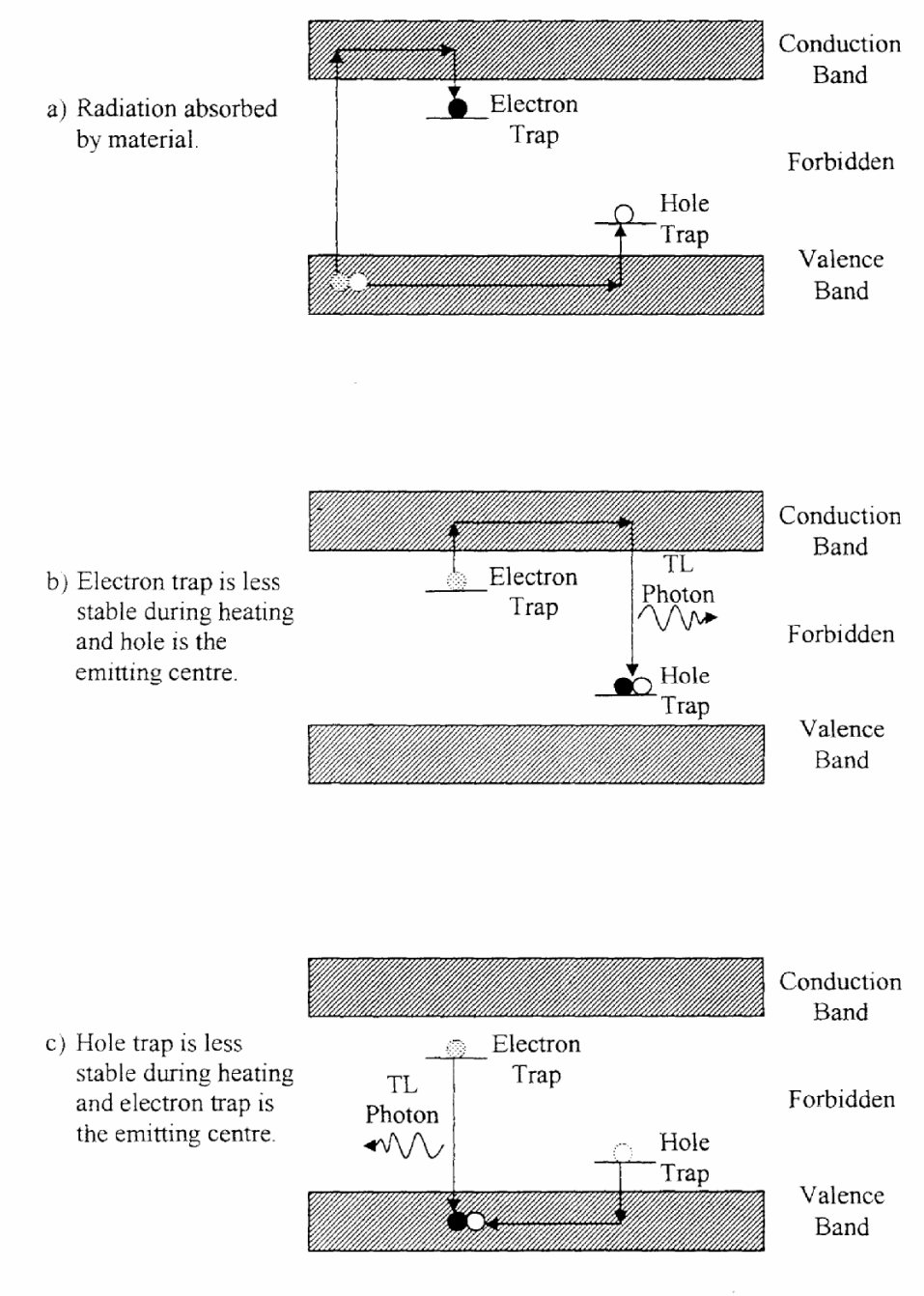

Figure 2.13 Schematic band model for thermolummescence.

There are two ways that the TL photon can be emitted, depending on the relative stability of the electron trap or hole trap. First, the electron trap maybe less stable than the hole trap, resulting in it being raised to conduction band , and become a photon emitting center for the TL photon. Secondly, the hole traps may be less stable than the

electron trap, it will then wander through the valence band until it eventually recombines with an electron trap, thus emitting a TL photon. TL can be used as a dosimeter and can be used to estimate the age of rocks and pottery. Lithium Fluoride (LiF:Mg is the most used as a dosimeter for recording the external dose.

Lithium Fluoride and Calcium Fluoride are the most popular dosimeters used. Lithium Fluoride (LiF) has activators such as magnesium (Mg) or titanium (Ti) this impurities make the dosimetry more active. LiF chip has dimensions of $3.2mm \times 3.2mm \times 0.9mm$. The trading name of Lithium Fluoride dosimeter is TLD100, TLD600 and TLD700 these differences came from the percentage ^{6}Li and ^{7}Li inside the phosphors.

2.10.2 Annealing

The original TLD sensitivity has to be recovered after irradiation and readout so, it is necessary to anneal the TLDs. Unfortunately, the TLD sensitivity is dependent on the details of the anneal cycle, so good control of the anneal cycle is important. Various annealing cycles have been proposed over the years, for different types of dosimeters.

Before the dosimeter is used again, its memory has to be erased so, annealing can be assumed the most important step in TL because this step erase the dosimeter memory and make it ready to be used to measure a new absorb dose. The annealing process is carried out inside a furnace and selection of suitable temperature and time for the dosimeter to be hold inside the furnace is the critical point in annealing. If new material is used as a dosimeter for a first time, it is necessary to perform at the first an annealing study which can be done as following:

- irradiate 10 TLDs samples to a test dose in the range of the field application.
- Anneal the irradiated samples at a given temperature (eg., $300^{\circ}C$) for a given period of time (e.g., 30 minutes).
- Read the samples.

- Repeat the three steps above increasing the annealing temperature of $50^{\circ}C$ each time up to the maximum value at which the residual TL (background) will remain constant as the temperature increase.
- Plot the data as shown in (Fig.2.14). as it can be observed , after a threshold temperature value T_c, the residual TL signal remains constant.
- Repeat now the procedure , keeping constant the temperature at the value T_c and varying the annealing time by steps of 30 minutes and plot the results. The plot should be similar to the previous one.
- Choose now the best combination of temperature and time.[9]

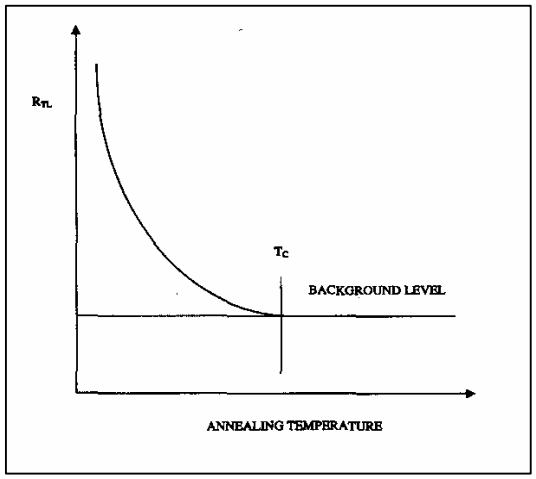

Figure 2.14. TL intensity Vs annealing temperature.

For the dosimeter LiF:Mg,Ti (TLD100,600,700) there are many annealing cycles. The first one is a long cycle 1 hour at $400^{\circ}C$ + 20 hour at $80^{\circ}C$. The second annealing cycle is 1 hour at $400^{\circ}C$ + 2 hour at $100^{\circ}C$. The third one is a fast anneal 15 min at $400^{\circ}C$ + 10 min at $100^{\circ}C$.

2.11 Instruments for characterization of nano particles

It is not possible for the researchers and scientists to use normal equipments such as optical microscope for characterizing and exploring the structures, composition and properties of nanoscale wires. To understand the materials behavior, it is important to know the composition and microstructure for those materials in the highest level of

resolution. That high resolution can not be maintains by the traditional optical microscope because theoretically the maximum resolution that can be obtained with a light microscope is limited by the wavelength of the light which is used to probe the sample. In early twentieth century that problem was solved by using electrons. The electrons can be used like a beam of electromagnetic wave because electrons have both wave and particle properties. As a result of that many kinds of electron microscope were invented. Many analytical techniques such as transmission electron microscopy, scanning electron microscopy, energy dispersive x- ray spectroscopy and x- ray diffraction have successfully used to characterize the structure of nano particles.

2.11.1 Transmission electron microscopy (TEM)

The first Transmission electron microscopy was built by Ernst Ruska in the 1930s. (TME) can be defined as a technique in which a beam of electrons is transmitted through a thin specimen. That electrons beam interacts with the specimen as it passes through it and an image of specimen is created. The image can be magnified and focused by an objective lens and appears on an imaging screen, a fluorescent screen, monitor, or a layer of photographic film, or sensor such as CCD camera. (fig. 2.15). show a diagram of Transmission electron microscopy.

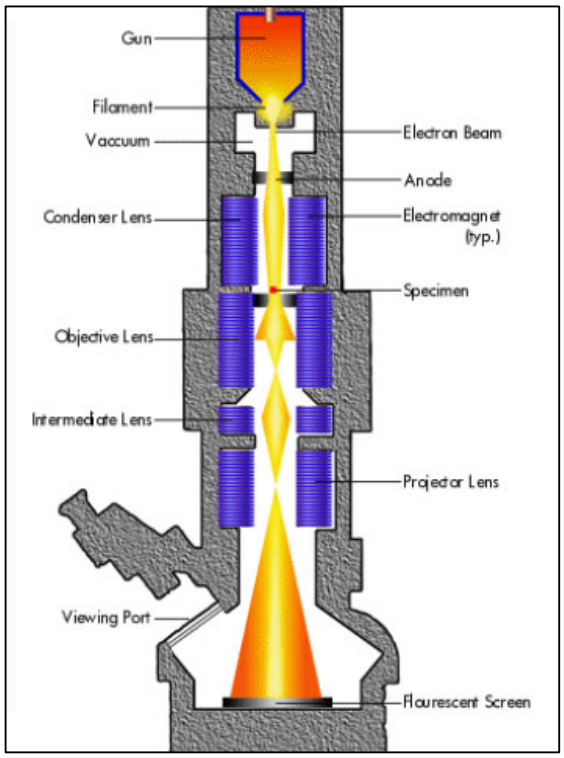

Figure. 2.15 Schematics diagram of Transmission electron microscopy

The working principle of TEM can be explained as following, an electron beam is produced through a filament which is made from a material that can produce a lot of electrons when it is heated an example for this material is tungsten. Electrical current is used to heat the filament and then the produced electron beam is accelerated due to the very high voltage between the cathode (filament) an the anode. The accelerated electron beam can be focused by using leans. The leans function as the optical leans in the normal light microscope which collect the light and focus it in one point, the same thing will happen for the electron beam by using the lens. Those lenses consist of electric or magnetic field. When the electron pass through the magnetic field it is effected by the force which make it deflect and by this method the electron beam can be focused in one point. The electrons beam has enough energy to be transmitted through the sample and some of electrons will scatter at different angles. The transmitted electron signal is greatly magnified by a series of electromagnetic lenses. The magnified transmitted

signal many be observed into two ways. The first way by direct electron imaging, this gives information about the microstructure of the material. The second way by electron diffraction imaging, this method is used to determine the crystallographic structure of the sample. That means TEM provide two methods in which the observation of specimen can be used. Those methods are diffraction mode and image mode. In diffraction mode, an electron diffraction pattern is obtained on the fluorescent screen, originating by the electron beam. The diffraction from the sample area is illuminated by the electron beam. The diffraction pattern is entirely equivalent to an X-ray diffraction pattern. The image mode produces an image of the illuminated sample area with different brightness. The image can contain contrast brought about by several mechanisms. Switch TEM between diffraction mode and image mode can be done as follows. The diffraction pattern and image are formed at the back focus plane and image plane of the objective lens. If the back focus plane is taken as the objective plane of the intermediate lens and projector lens, we will obtain the diffraction pattern on the screen. It is said that the TEM works in diffraction mode. If the image plane of the objective lens is taken as the objective plane of the intermediate lens and projector lens, we will form image on the screen and this is the image mode (fig. 2.16).

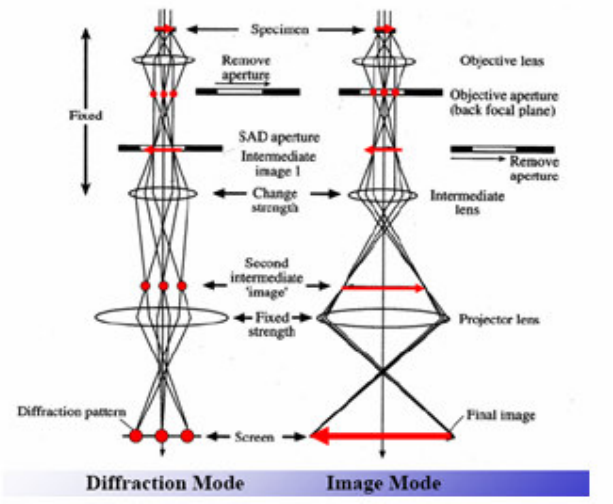

Figure. 2.16 Schematics diagram for Switching TEM between diffraction mode and image mode.

2.11.2 Scanning Electron Microscopy

In the scanning electron microscopy a focused high energy beam of electrons are used to get information about the sample including external morphology, chemical composition and crystalline structure of materials making up the sample. This kind of required electron beam can be maintained by the electron gun which emits electrons from the filament. Electron beam is accelerated and then be focused by electromagnetic leans. Before interacted with the sample, the electrons can be raster the sample surface by using a set of scanning coils. The electrons interact with few nanomters to several microns of the sample as a result of that different signals are produced such as secondary electrons, backscattered electrons, diffracted backscattered electrons and x-ray which carry information about the sample. Secondary electrons and backscattered electrons are detected by a special detector which produces light according to received electrons. A series of treatments are done for this light which finally produce an image for the sample which is displayed in a cathode ray tube. Diffracted backscattered electrons are used to determine crystal structures and characteristic x-ray is used for elemental analysis. (fig2.17)

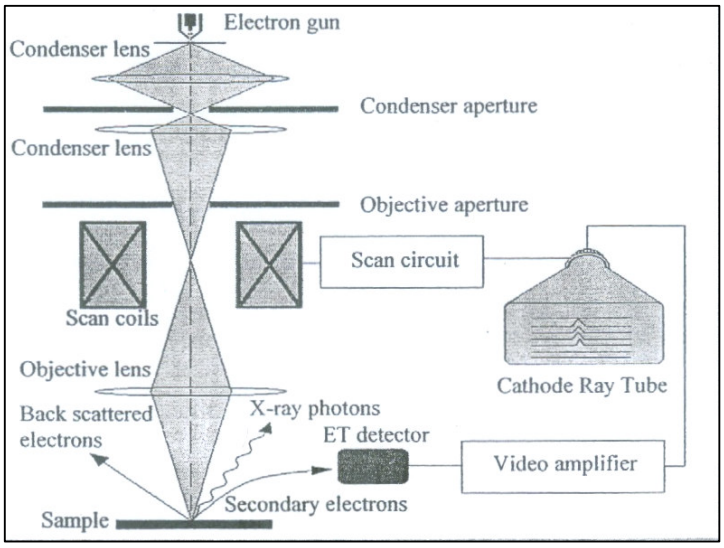

Figure. 2.17 Schematics diagram of a scanning electron microscope. [22].

2.11.3 Energy Dispersive x- ray Spectroscopy (EDS)

This instrument is attached with SEM but in this time the analysation is done by using x-ray emitted from the sample instate of using secondary electron. EDS analyze chemical compositions of a sample so, the compounds of sample can be known by this analytical technique. The working principle of EDS is similar to that of SEM technique except that x-ray are produced from the sample and received by a special detector which is consist of a thin silicon crystal doped with lithium with thin gold electrodes . (fig. 2.18). When X-ray photon hits the detector, it produces a large number of electrons and holes in the Si(Li) region. Electrons are then accelerated to the positive side, and holes to the negative side. Thus, a pulse of current is generated. The pulse current is proportional to the X-ray energy. Characterized x-ray energy is unique for each element so, the compounds which the sample contains can be known from EDS pattern as it is shown in. (fig. 2.19).

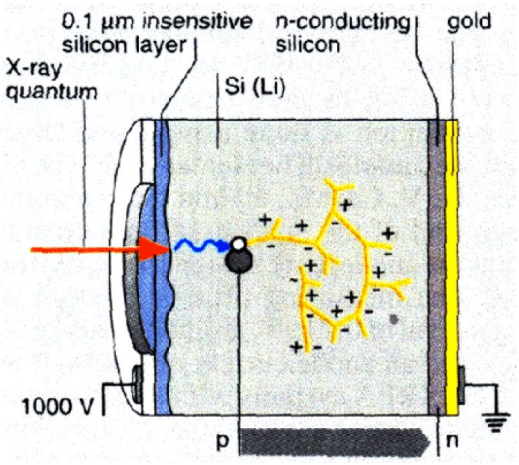

Figure 2.18 Electron dispersive x-ray spectrometer detector.

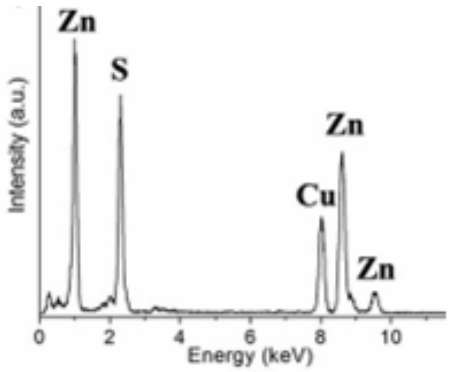

Figure 2.19 EDS pattern obtained from ZnS nano particles sample.

2.11.4 X- Ray Diffraction

X-ray has a wave length of order Angstroms which is equivalent to magnitude of atomic dimensions so; x-ray is suitable to make some investigation for the sample by using x-ray diffraction. Information about crystalline size, interlayer distance and chemical composition can be provided by using this technique. The principle of this technique is based in Bragg's law, when a beam of x-ray is focused to a crystalline compound this beam is scattered and by taking the resultant constructive Interference pattern and take in the account the direction and intensity of the diffracted beams, the unknown sample can be easily achieved by comparing its x-ray diffractogram with an internationally recognized database.

According to Bragg's law the intensity of scattered waves is at maxima if the bath difference is equal to integral of wavelength that mean ($2d \sin\theta = n\lambda$) where (d) is the spacing between the deferent planes in the crystal. (θ) is the angle between the incident x-ray and the surface. The diffraction happens if the crystals are parallel to the surface so, it is necessary to rotate the sample so that the Bragg's law is satisfied and record more than one maxima at deferent angles (θ) . When the sample is rotated and the Bragg's law is satisfied for some θ's the constructive scattered x-ray has to be sure that is collected by the detector. That can be done by rotating the sample by a constant angular velocity ω so the angle of incidence of the primary beam changes and at the same time rotating the detector by angular velocity equal to 2ω hence, the scattering angle is always twice of the temporary incidence angle so, the scattering angle equals 2θ . (fig. 2.20).

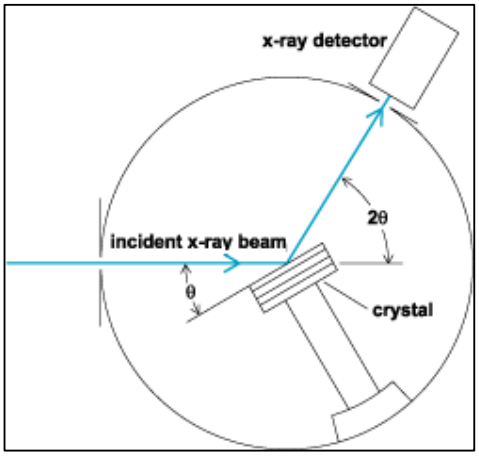

Figure 2.20 Schematic of Bragg spectrometer.

XRD pattern of synthesized ZnS nano particles on a Si substrate is illustrated in (fig2.21) . By using miller indices the distance between planes (d) can be calculated from the equation

$$d(h,k,l) = \frac{a}{\sqrt{h^2 + k^2 + l^2}}$$

For the miller indices $h = 1, k = 0, l = 0$ the atomic distance is equal to distance between plans so, the (d) for this plane can be calculated from the Bragg's equation $2d \sin\theta = n\lambda$ which is also equal to (a). $a = d = \frac{n\lambda}{2\sin\theta}$

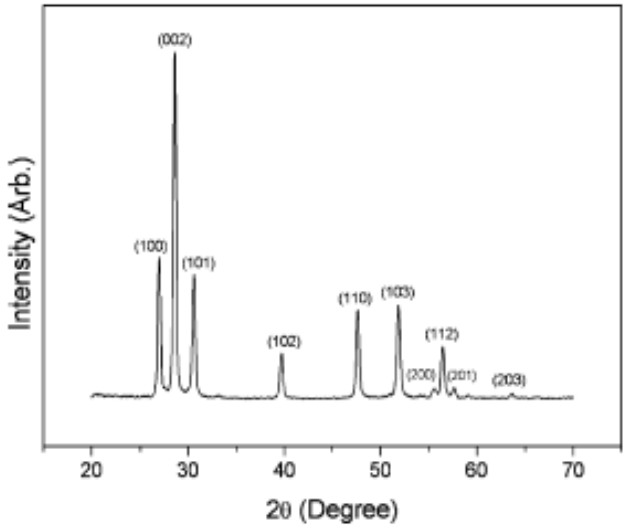

Figure 2.21 XRD pattern of synthesized ZnS nano particles on a Si substrate

References:

[1] Ji Liu " Synthesis and Characterization of GaN/ZnS Nanomaterials" (CITY UNIVERSITY OF HONG KONG, 2004).

[2] SIU KEUNG CHAN " MBE-VLS grown ZnSe and ZnS nanowires growth mechanisms and photoluminescence properties" (The Hong Kong University of Science and Technology 2007)

[3] H.Hartmann,R.Mach and B.Selle, "Wide Gap II-VI Compounds as Electronic Materials",in"current Topics in Materials Science", edit by E.Kaldis, Vol,a,(North-Holloand Pablishing Company,1982).

[4] C.H.L,Goodman,"Crystal Growth Theory and Techniques".Vol.1,(Plenum Publishing Company,LTD,1974)

[5] B.Segall and D.T.F Marple, Physics and Chemistry of II-VI compounds,(North Holand,Amsterdam,1967).

[6] A.Pryor William. "Mechanisms Of Sulfur Reactions"(McGRAW-HILL BOOK Company,INC. New YORK,1962)

[7] A.Muller and B.Krebs "Studies In Inorganic Chemistry,Sulfur"(Elsevier Science Publishers B.V,AH Amsterdam,1984).

[8] James B. Calvert (2003) the element that like to form chains retrieved 8/2/2009 from http://mysite.du.edu/~jcalvert/phys/sulphur.htm

[9] Richard Beatty. " The Elements, sulfur ". (Marshall Cavendish, 2000).

[10] K.K.Chatterjee. "Uses Of Metals and Metallic Minerals" (New Age International(p) Ltd, New Delhi, 2007).

[11] N.N Greenwood and A.Earnshaw "Chemistry of the Elements" (Pergamon Press, 1997).

[12] H.Yufeng, M.Guowen, W.Zhong,Y.Changhui and Zhang."periodically twinned nanowires and polytypic nanobelts of ZnS: the role of mass diffusion in vapor-liquid-solid growth",Nano Lett,Vol.6, No.8,2006.

[13] L. Wang Zhong and M Daniel, Growth of anisotropic one-dimensional ZnS nanostructures. Chem.16, 2006.

[14] W. Kelsall Robert, W. Hamley Ian and G. Mark "Nanoscale Science and Technology" (John Wiley & Sons Ltd, England. 2005)

[15] C.N.R.Rao,A.Muller and A.K.Cheetham." The Chemistry of Nanomaterials, synthesis, properties and Applications. Vol.1",(Willy-VCH Verlag Gmbh and Co.KgaA, 2004).

[16] Cao Guozhong, "Nanostructures and Nanomaterials, synthesis,properties and applications",(imperial collage press 57 shelton street covent gardn London WC2H 9HE, 2004).

[17] X.M Meng et al / chemical physics letters 382 (2003) 434-438

[18] H. Moon et al / Materials Research Bulletin 41 (2006) 2013-2017

[19] X. Zhang et al / physica E 28 (2005) 1-6

[20] H. Xintang and T. Ming / journal of Applied Sciences., 6(14): 2940-2943, 2006.

[21] G.H. YUE / journal Appl. Phys. A 84, 409–412 (2006)

[22] C.L. Cheng " synthesis of carbon nanotybe using hot filament chemical vapour deposition technique " (university of Malaya, 2007).

[23] A.Yazici, O.Mustafa, B.Mctin and R.Kayali "determination of the trapping parameters of ZnS thin films developed by chemical spraying technique", Turk J Phys 26(2002),277, 282.

(ABO-Hassan 1997) K.M.M . ABO-Hassan, " optical and electrical characteristics of E-beam evaporated (ZnS_xSe1-x) thin films, (institute of postgraduate studies and research university of Malaya kuala Lumpur 1997)

CHAPTER 3

Experimental Setup

3.1 Experimental Setup

A lot of methods are used to synthesis ZnS nano particles. Chemical precipitation is widely used for the preparation of colloidal nanoparticles. Cluster formation is very less in this method compared to the other methods. Simple thermal chemical reaction vapor transport deposition method is another method to produce nanoparticles. In this experiment the two methods were used.

3.1.1 Synthesis of ZnS nano particles chemical precipitation method.

In this work ZnS:Mn nanoparticles were synthesized by using three chemical compounds which are Zinc sulfate, Sodium sulfide and Manganese sulfate. The solutions were prepared in distilled water with concentrations of 0.5126M, 0.069M and 1M respectively. The previous concentrations were obtained by dissolved 22.11g of $ZnSO_4$ in 150 ml of distilled water, 0.47g of Na_2S in 50ml of distilled water and 1.7g of $MnSo_4$ in 10ml of distilled water. The solutions were first refluxed for an hour separately. So, 150ml of $ZnSO_4$,50 ml of Na_2S and 10 ml of $MnSO_4$ were prepared.

Three kinds of different samples had been synthesized in the test. Sample number one was prepared by adding 50 ml of $ZnSO_4$ to 6 ml of Na_2S which was continuously refluxed to get a colloidal form of ZnS. The colloidal sample was refluxed for 20 min at 80°C for uniform distribution of the particles. 1 ml of $MnSO_4$ was then added into 50 ml

ZnS colloid (which is already prepared). The colloidal sample was again stirred for another 30 min at 80°C. Then this colloidal was filtered out and washed with distilled water and ethanol for removing the additional impurities formed during the preparation process. The filtrate was dried at 100°C for 4 h. The previous steps for sample number one were repeated two more times for other samples but with $MnSO_4$ concentration of 2M and 3M.

. The replacement reaction can be written as follows:

$$ZnSo_4 \leftrightarrow Zn^{2+} + So^{2-}$$

$$N(Zn^{2+} + Na_2S) \leftrightarrow (ZnS)_N + 2N(Na^+)$$

The prepared product was characterized and analyzed using scanning electron microscopy (SEM) and energy dispersive x-ray spectroscopy (EDX).

3.1.2 Synthesis of ZnS nanoparticels by vapor transport deposition method

ZnS nanostructures are grown on silicon (100) wafers by using of a simple thermal chemical reaction vapor transport deposition method by heating the zinc and sulpher powders. There is no other metal catalyst in the process. The experimental system consists of a horizontal tube furnace (110 cm long), temperature controller, gas supply and control system. One side of the horizontal tube was connected to a vacuum pump and its other end is linked with gas supply and control system (fig 3.1). The source materials are high-purity of Zn (98%) and S (98%) powders in molar ratio of 1:1. In the experimental process, small quartz boat (2.5 cm diameter, 10 cm long) was placed into the horizontal tube and pushed to the center of the furnace (which has the maximum point of temperature). Silicon substrate pieces (Si [100] were place 2 cm downstream from the center. The reaction was heated at $700^{\circ}C$ in the center and the temperature of the substrate region was about $500^{\circ}C$ due to the temperature gradient. The Ar gas (99.9%) had been introduced as the carrier with flow rate was 60 standard cubic centimeters per minute (s.c.c.m). The heated at $700^{\circ}C$ was continued for 15 min.

Finally the furnace was turned off and the quartz tube was cooled down to room temperature. White color products were formed on the surface of the silicon wafer.

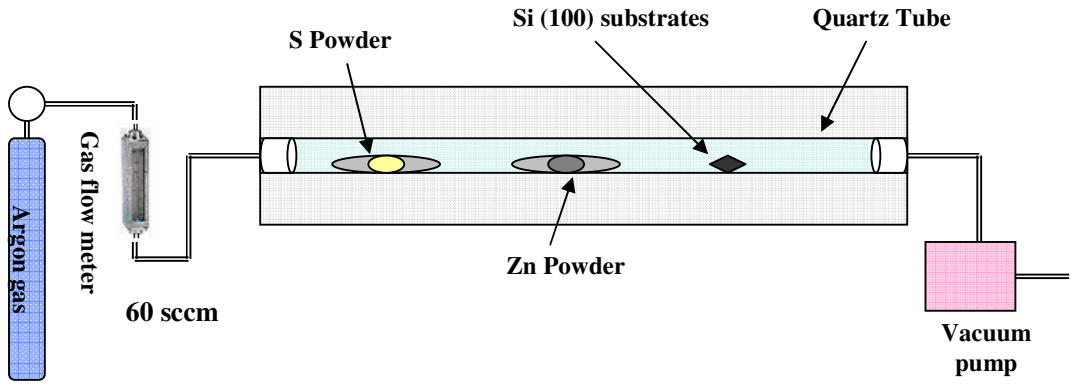

Fig. 3.1 Schematics showing the synthesis of ZnS nanoparticels by vapor transport deposition method

CHAPTER 4

Characterization

4.1 ZnS powder and ZnS nano particles (SEM image)

The morphology and chemical composition of ZnS:Mn particles synthesized by chemical precipitation were characterized by high resolution scanning electron microscopy FESEM, XRD and EDX . (Fig. 4.1) and (Fig.4.2) shows FESME image of commercial ZnS powder and ZnS nano particles respectively.

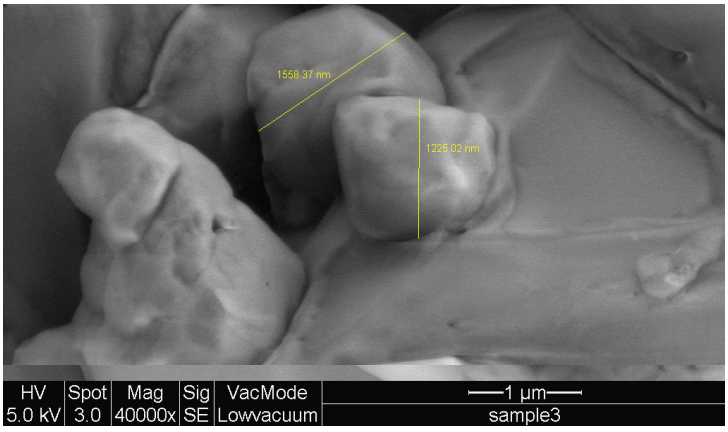

Figure 4.1 SEM image of commercial ZnS powder

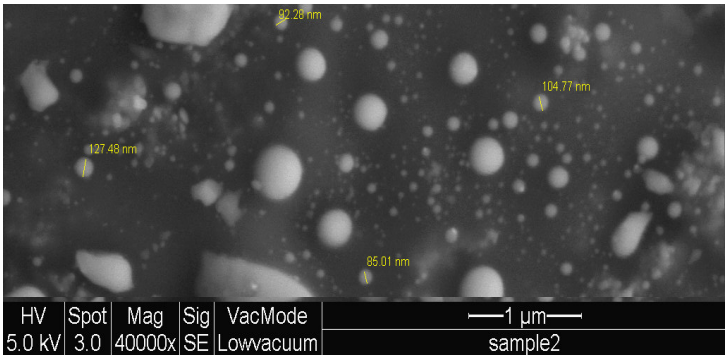

Figure 4.2 SEM image of ZnS nano crystal

It can be seen that the obtained products consist of particles with the dimension about 85–150nm, Compared with the size of ZnS commercial particles which have dimension of order of microns.

4.2 EDX spectra of ZnS powder and ZnS nano particles

The EDX spectra indicate that the particles were composed of Zn, S, and Mn as shown in Fig.4.3. and Fig 4.4.

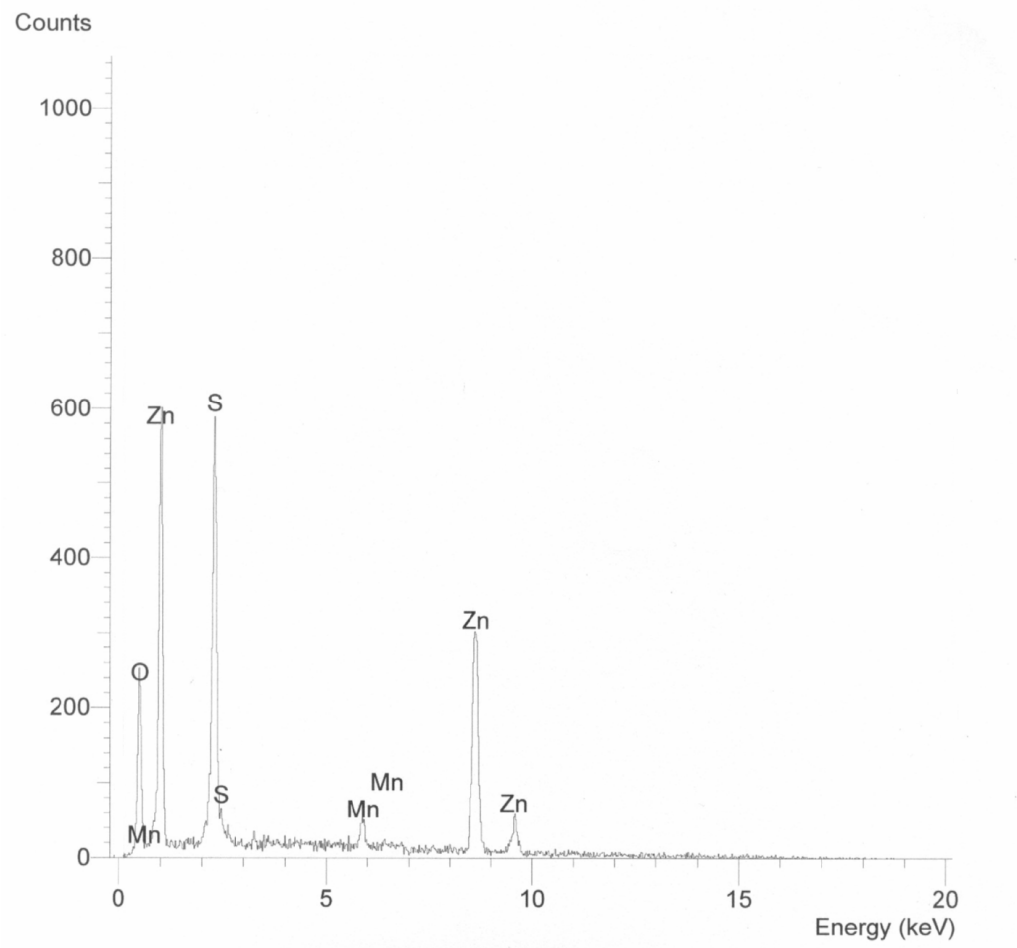

Figure 4. 3 EDX of ZnS nano particles

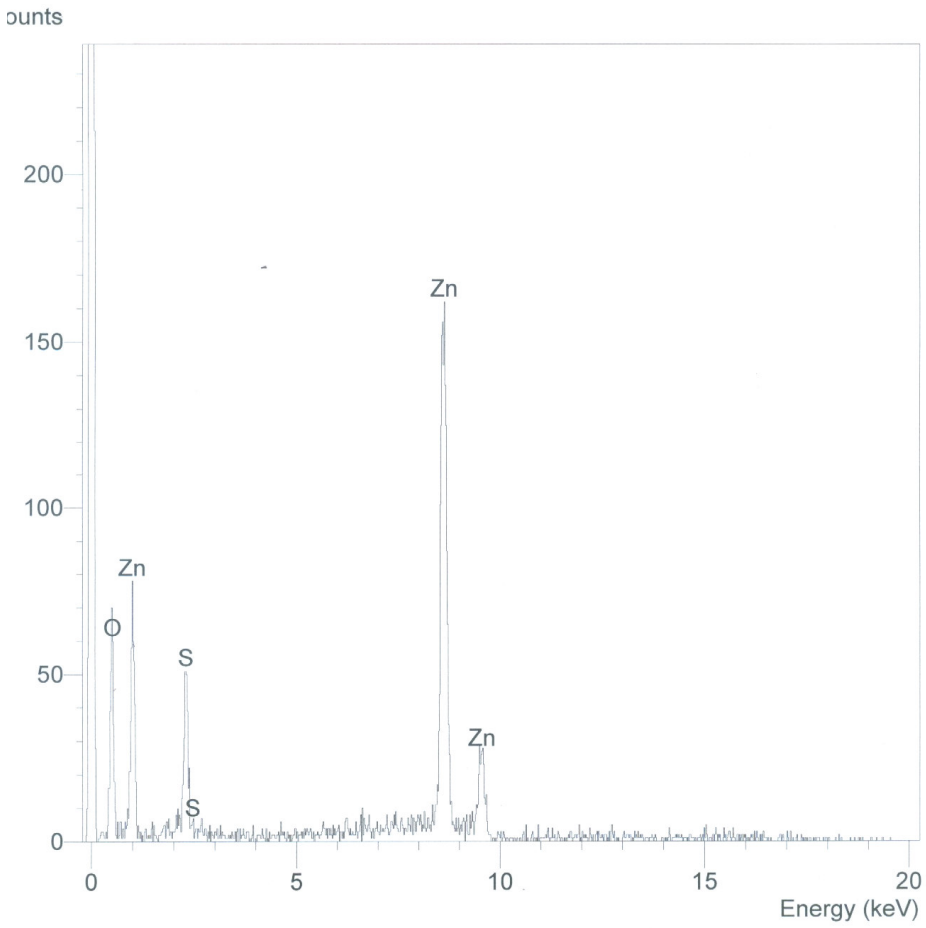

Figure 4.4 EDX of ZnS commercial powder

By comparing the compounds of commercial ZnS and ZnS nano particles, it can be seen that in the two samples the oxygen is existed.

4.3 XRD patterns of ZnS powder and ZnS nano particles

Fig.4.5 shows XRD patterns of a commercial ZnS powder and the ZnS: Mn nano particles. The peaks are observed at 2θ values of 26.3◦, 46.2◦, and 56.9◦, which correspond to the (111), (220), and (331) planes of cubic ZnS, respectively.

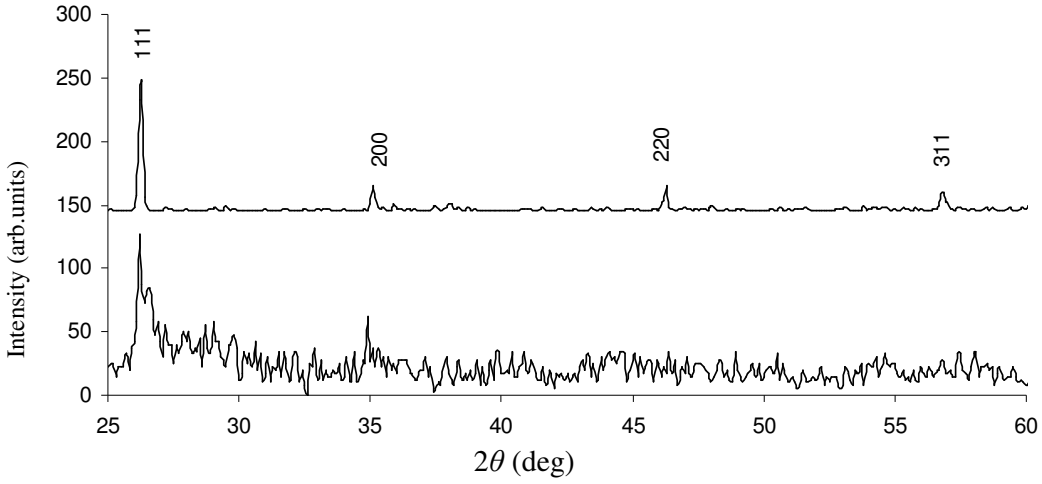

Figure 4.5. XRD patterns of ZnS powder (top) and ZnS:Mn nano particles (bottom)

CHAPTER 5

Results and Analysis

5.1 ZnS nano particles synthesis by chemical precipitation method

Five samples were prepared to investigate the TL properties of ZnS:Mn nanophoshor each sample has a mass of 30 mg. The first three samples have Mn concentration of 1M,2M and 3M respectively. Sample four does not contain Mn and sample five is a commercial ZnS powder.

The Annealing process takes place in a furnace of model Vulcan 3-400HTA. The furnace was programmed so that the samples were heated gradually to $500^{\circ}C$, $300^{\circ}C$ and $100^{\circ}C$. Each temperature was kept constant for 30 minutes. The heating rate was $40^{\circ}C/\min$. Then the samples were exposed to a gamma ray by using Gamma cell 220 which uses ^{60}Co as a source of gamma (γ) rays. The samples were exposed to a dose equal to 18 Gy, 36 Gy, 54 Gy, 72 Gy and 90 Gy then the thermoluminescence properties were studied by using Harshaw 3500 reader.

Fig. 5.1 and Fig 5.2 shows the glow curve of commercial ZnS powder and ZnS nanophosphors after they are irradiated by gamma ray with a dose equal to 54 Gy. By making comparison between the two graphs, it can be seen that the glow curve of ZnS nanophosphors shows a good clear peak compared with the glow curve of commercial ZnS powder which shows no fine clear peaks. That's means decreasing the particle size of ZnS gives a good emission of TL intensity.

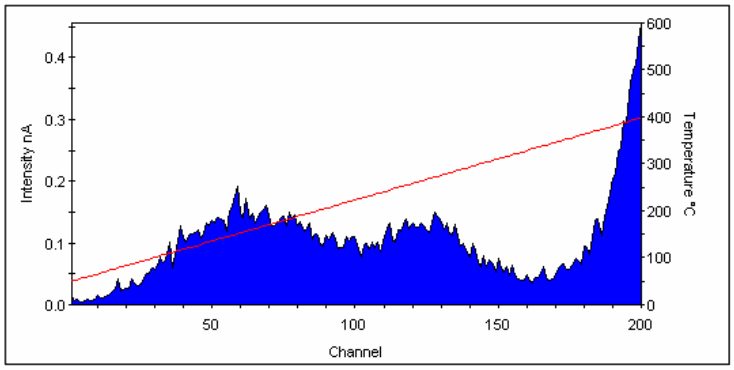

Figure .5.1 TL glow curve of commercial ZnS powder

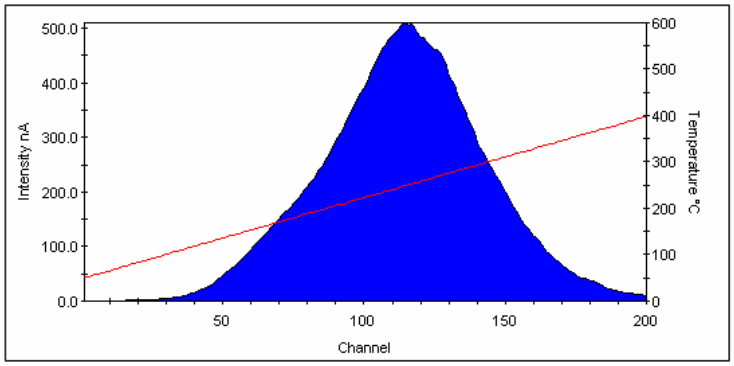

Figure 5.2 TL glow curve of ZnS nano particles

5.2 calculating the absorbed dose

The exposure time can be calculated according to the required absorbed dose by using the following equation:

$$\exp ouser \quad time(\sec ond) = \frac{absorbed \quad dose(Gy)}{dose \quad rate(Gy/\sec ond)}$$

The previous equation can be rewritten as following

$absorbed \quad dose(Gy) = dose \quad rate(Gy/\sec ond) \times \exp ouser \quad time(\sec ond)$ so, by this equation the required absorbed dose can be obtained.

The exposure rate of ^{60}Co is not constant so, the radiation dose rate will decrease every month as shown in the table (5.1). The exposure rate can be calculated for any time (t) by using the equation

$D_t = D_\circ e^{-\lambda t}$ where $\lambda = 4.1681 \times 10^{-9} s^{-1}$, $D_\circ = 0.525 Gy/\sec$

2005	
Time (month)	Dose Rate (Gy / sec)
January	0.15957
February	0.15789
March	0.15618
April	0.15450
May	0.15284
June	0.15120
July	0.14958
August	0.14797
September	0.14638
October	0.14481
November	0.14325
December	0.14171

2006	
Time (month)	Dose Rate (Gy / sec)
January	0.14019
February	0.13868
March	0.13719
April	0.13572
May	0.13426
June	0.13282
July	0.13139
August	0.12998
September	0.12858
October	0.12720
November	0.12583
December	0.12448

2007	
Time (month)	Dose Rate (Gy / sec)
January	0.12314
February	0.12182
March	0.12051
April	0.11922
May	0.11794
June	0.11667
July	0.11542
August	0.11418
September	0.11295
October	0.11174
November	0.11054
December	0.10935

2008	
Time (month)	Dose Rate (Gy / sec)
January	0.10817
February	0.10701
March	0.10586
April	0.10472
May	0.10359
June	0.10248
July	0.10138
August	0.10029
September	0.09921
October	0.09814
November	0.09709
December	0.09605

2009	
Time (month)	Dose Rate (Gy / sec)
January	0.09502
February	0.09400
March	0.09299
April	0.09199
May	0.09100
June	0.09002
July	0.08905
August	0.08809
September	0.08714
October	0.08620
November	0.08527
December	0.08435

2010	
Time (month)	Dose Rate (Gy / sec)
January	0.08344
February	0.08254
March	0.08165
April	0.08077
May	0.07990
June	0.07904
July	0.07819
August	0.07735
September	0.07652
October	0.07570
November	0.07419
December	0.07339

Table 5.1. ^{60}Co dose rate

5.3 The thermoluminescence properties of manganese doped ZnS nanophoshor

5.3.1 ZnS commercial powder

exposure time(sec)	dose rate(Gy/sec)	absorb dose(Gy)	TL intensity (nC)
195	0.09199	18	4.9
391	0.09199	36	5.2
585	0.09199	54	7.3
780	0.09199	72	8.1
975	0.09199	90	11.0

Table 5.2 exposure time, dose rate , absorb dose and TL intensity of ZnS commercial powder

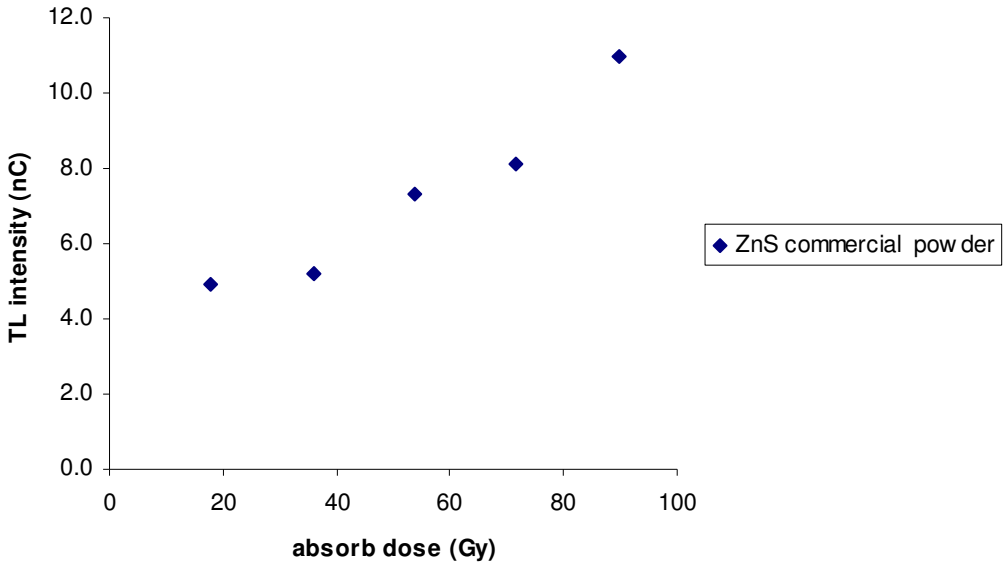

Figure 5.3 TL intensity vs absorb dose of ZnS commercial powder

5.3.2 ZnS nanophoshor without manganese

exposure time(sec)	dose rate(Gy/sec)	absorb dose(Gy)	TL intensity (µC)
195	0.09199	18	1.3
391	0.09199	36	3.2
585	0.09199	54	5.8
780	0.09199	72	7.2
975	0.09199	90	11.3

Table 5.3 exposure time, dose rate , absorb dose and TL intensity of ZnS nanophoshor without manganese

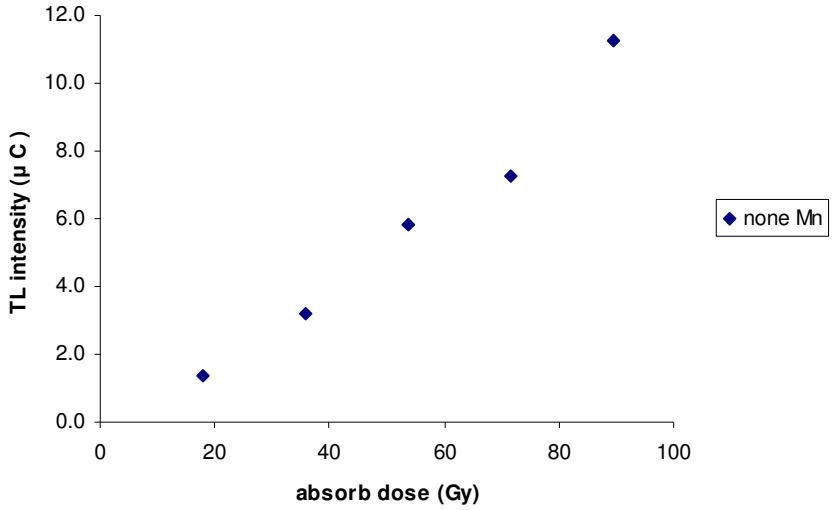

Figure 5.4 TL intensity vs absorb dose of ZnS nanophoshor without manganese

5.3.3. ZnS nanophoshor doped with 1mol of manganese sulfate

exposure time(sec)	dose rate(Gy/sec)	absorb dose(Gy)	TL intensity (μC)
195	0.09199	18	2.0
391	0.09199	36	4.9
585	0.09199	54	9.9
780	0.09199	72	13.2
975	0.09199	90	19.7

Table 5.4 exposure time, dose rate , absorb dose and TL intensity of ZnS nanophoshor doped with 1mol of manganese sulfate

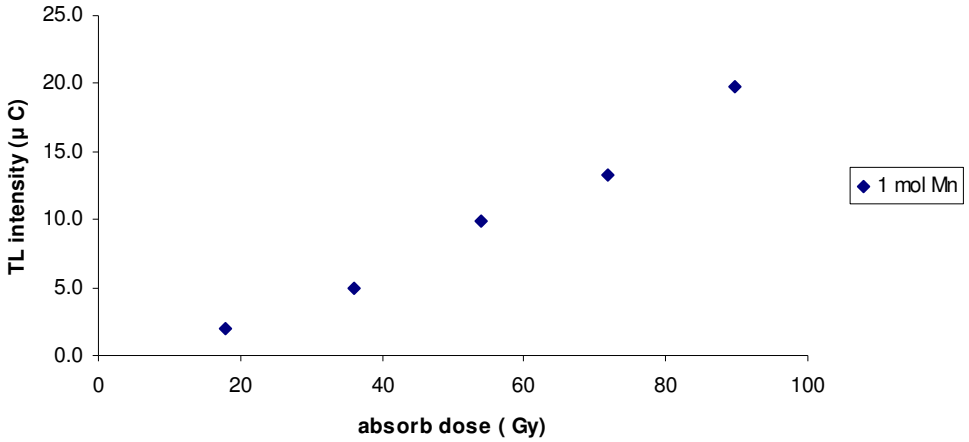

Figure 5.3 TL intensity vs absorb dose of ZnS nanophoshor doped with 1mol of manganese sulfate

5.3.4 ZnS nanophoshor doped with 2mol of manganese sulfate

exposure time(sec)	dose rate(Gy/sec)	absorb dose(Gy)	TL intensity (μC)
195	0.09199	18	2.3
391	0.09199	36	6.1
585	0.09199	54	11.7
780	0.09199	72	15.7
975	0.09199	90	20.7

Table 5.5 exposure time, dose rate , absorb dose and TL intensity of ZnS nanophoshor doped with 2mol of manganese sulfate

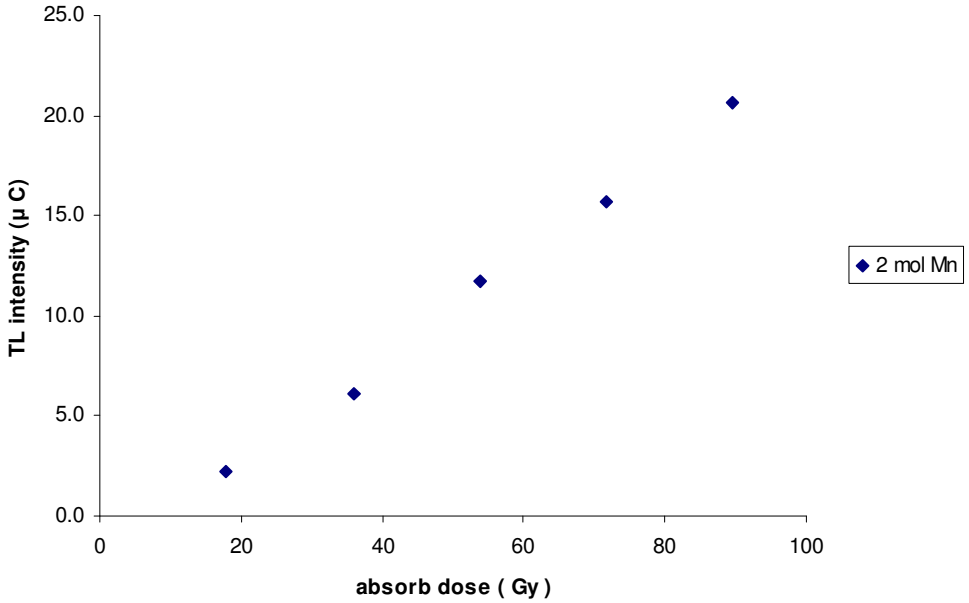

Figure 5.6 TL intensity vs absorb dose of ZnS nanophoshor doped with 2mol of manganese sulfate

5.3.5 ZnS nanophoshor doped with 3mol of manganese sulfate

exposure time(sec)	dose rate(Gy/sec)	absorb dose(Gy)	TL intensity (µC)
195	0.09199	18	3.2
391	0.09199	36	6.3
585	0.09199	54	10.5
780	0.09199	72	12.4
975	0.09199	90	16.1

Table 5.6 exposure time, dose rate , absorb dose and TL intensity of ZnS nanophoshor doped with 3mol of manganese sulfate

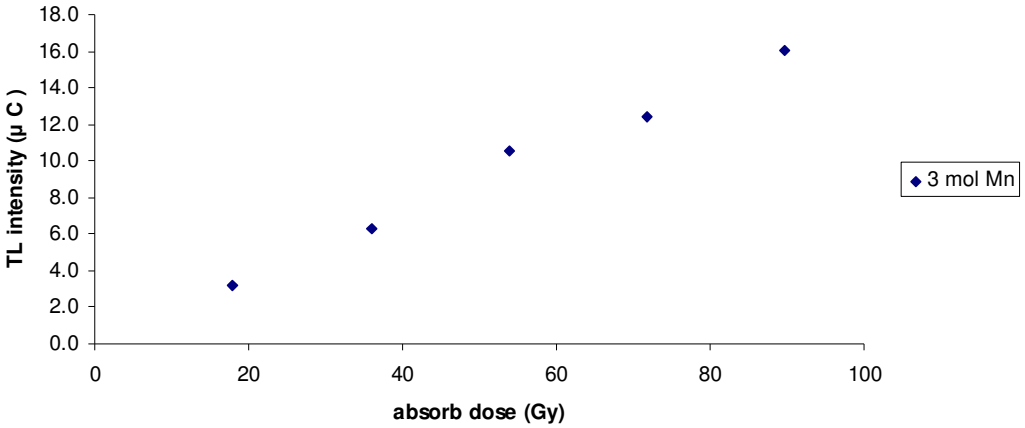

Figure 5.7 TL intensity vs absorb dose of ZnS nanophoshor doped with 3mol of manganese sulfate

exposure time(sec)	dose rate(Gy/sec)	absorb dose(Gy)	TL intensity (μC) 1 mol Mn	2 mol Mn	3 mol Mn	none Mn
195	0.09199	18	2.0	2.3	3.2	1.3
391	0.09199	36	4.9	6.1	6.3	3.2
585	0.09199	54	9.9	11.7	10.5	5.8
780	0.09199	72	13.2	15.7	12.4	7.2
975	0.09199	90	19.7	20.7	16.1	11.3

Table 5.7 exposure time, dose rate , absorb dose and TL intensity of ZnS doped with different Mn concentrations

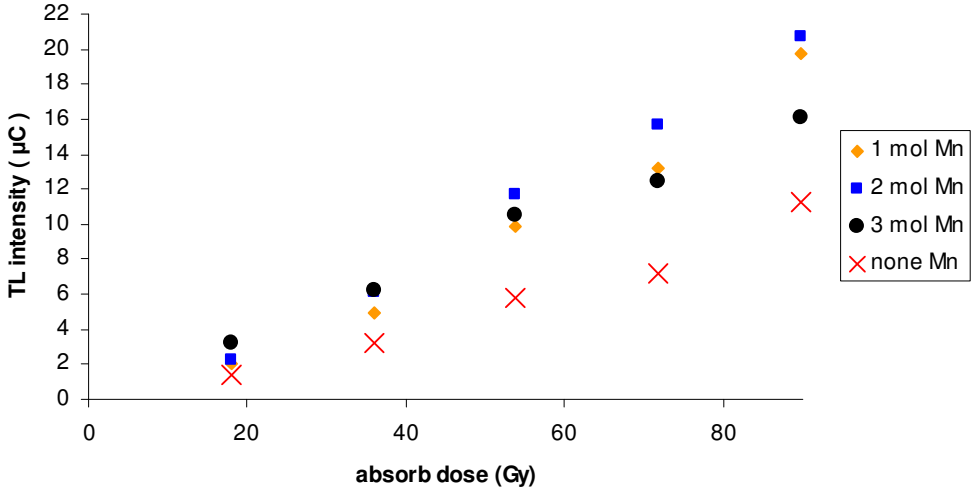

Figure 5.8 TL intensity vs absorb dose of ZnS doped with different Mn concentrations

As it is obvious in (fig.5) the TL response against absorbed dose shows linearity and increasing Mn concentration enhances the TL response. The amount of Mn concentration of 2 mole gives the best emission of TL but as the concentration is increased, the TL response is decreased. That is because ZnS becomes more conductivity as the Mn concentration increase. Semiconductors and insulators are good thermoluminescence materials unlike conductive materials which are poor thermoluminescence materials so; adding Mn in ZnS should be in a certain amount which increases TL properties of ZnS without changing it to conductive material.

5.4 Fading properties of manganese doped ZnS nanophoshor

5.4.1 Fading of ZnS commercial powder

exposure time(sec)	dose rate(Gy/sec)	absorb dose(Gy)	fading	TL intensity (nC)
591	0.091	53.8	No fading	9.4
			1 hour	9.1
			2 hour	7.9
			3 hour	8.3
			4 hour	7.1
			1 day	5.2
			2 day	5.1
			3 day	4.4
			4 day	3.9

Table 5.8 exposure time, dose rate , absorb dose , fading and TL intensity of ZnS commercial powder

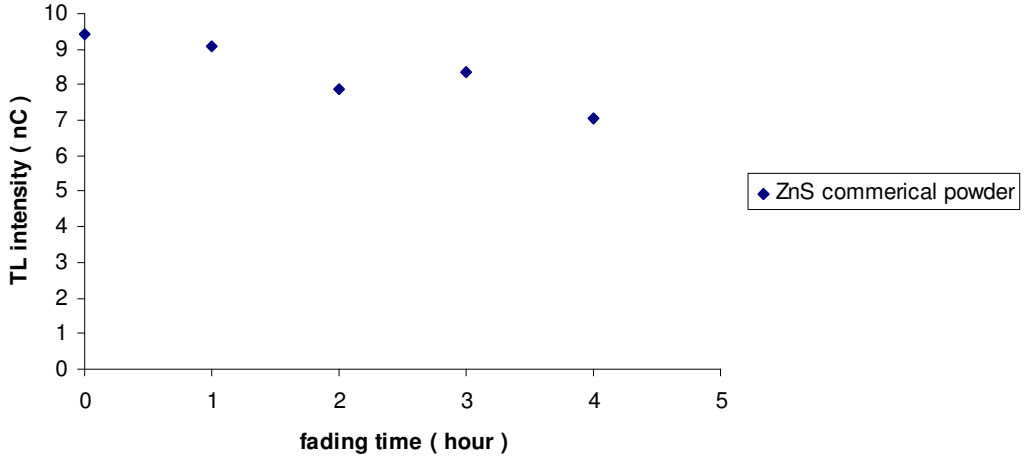

Figure 5.9 TL intensity vs fading time (hour) of ZnS commercial powder

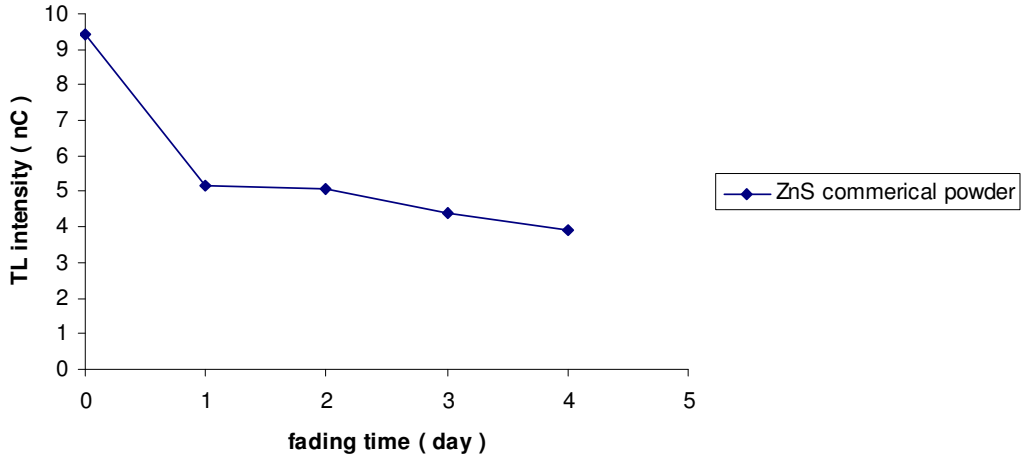

Figure 5.10 TL intensity vs fading time (day) of ZnS commercial powder

5.4.2 Fading of ZnS nanophoshor without manganese

exposure time(sec)	dose rate(Gy/sec)	absorb dose(Gy)	fading	TL intensity (µC)
591	0.091	53.8	No fading	6.12
			1 hour	4.7
			2 hour	4.2
			3 hour	3.7
			4 hour	3.1
			1 day	3.6
			2 day	2.8
			3 day	2.8
			4 day	2.2

Table 5.9 exposure time, dose rate , absorb dose , fading and TL intensity of ZnS nanophoshor without manganese

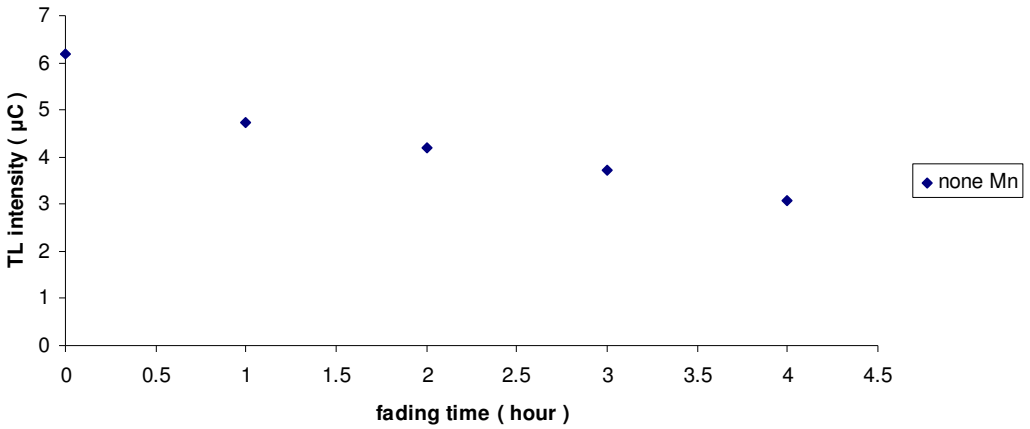

Figure 5.11 TL intensity vs fading time (hour) of ZnS nanophoshor without manganese

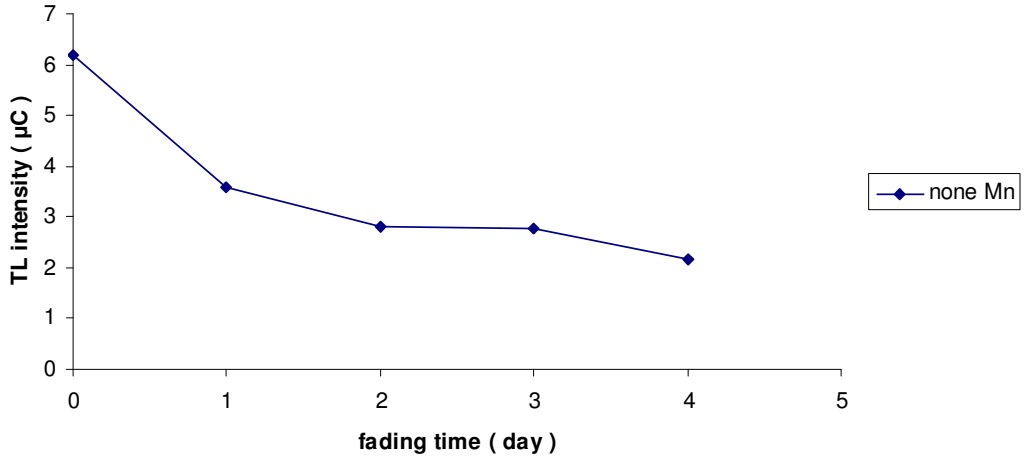

Figure 5.12 TL intensity vs fading time (day) of ZnS nanophoshor without manganese

5.4.3. Fading of ZnS nanophoshor doped with 1mol of manganese sulfate

exposure time(sec)	dose rate(Gy/sec)	absorb dose(Gy)	fading	TL intensity (µC)
591	0.091	53.8	No fading	12.9
			1 hour	11.3
			2 hour	10.6
			3 hour	8.2
			4 hour	5.2
			1 day	7.7
			2 day	7.6
			3 day	7.0
			4 day	3.5

Table 5.10 exposure time, dose rate , absorb dose , fading and TL intensity of ZnS nanophoshor doped with 1mol of manganese sulfate

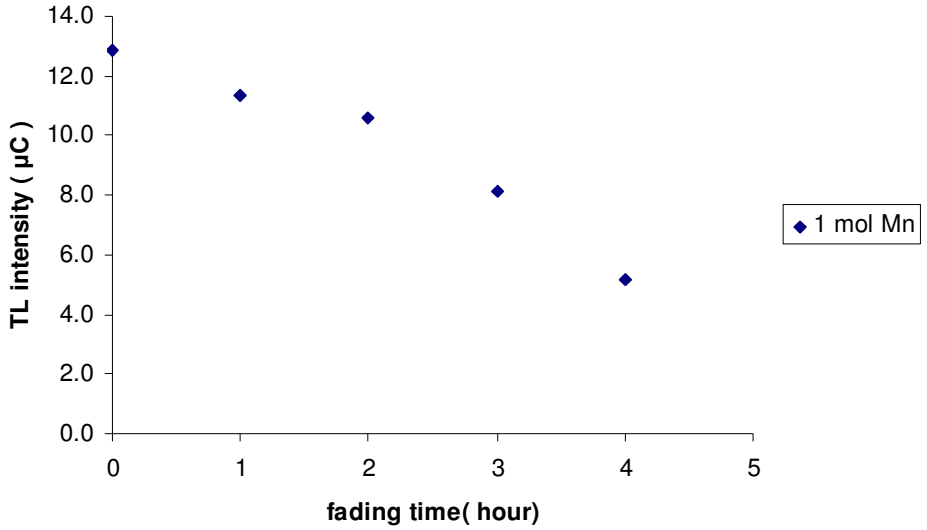

Figure 5.13 TL intensity vs fading time (hour) of ZnS nanophoshor doped with 1mol of manganese sulfate

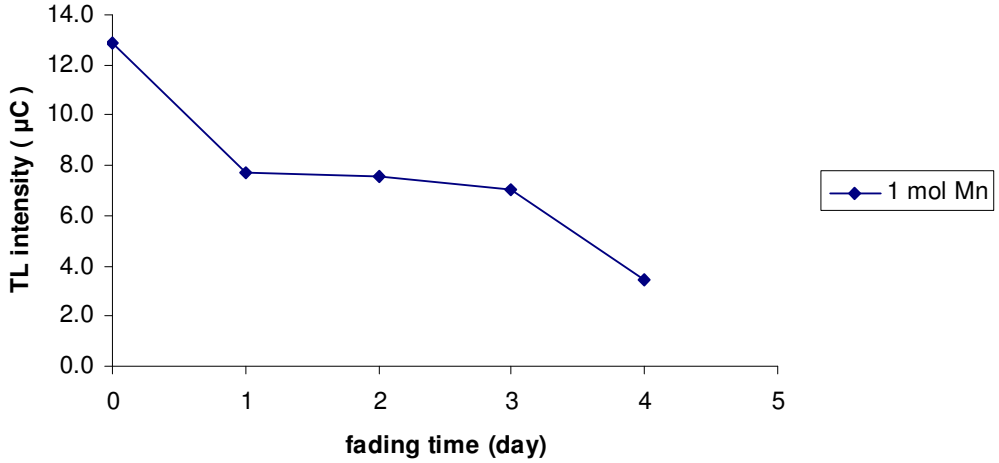

Figure 5.14 TL intensity vs fading time (day) of ZnS nanophoshor doped with 1mol of manganese sulfate

5.4.4. Fading of ZnS nanophoshor doped with 2mol of manganese sulfate

exposure time(sec)	dose rate(Gy/sec)	absorb dose(Gy)	fading	TL intensity (µC)
591	0.091	53.8	No fading	12.8
			1 hour	11.3
			2 hour	10.8
			3 hour	8.9
			4 hour	5.3
			1 day	7.7
			2 day	7.3
			3 day	6.7
			4 day	3.7

Table 5.11 exposure time, dose rate , absorb dose , fading and TL intensity of ZnS nanophoshor doped with 2mol of manganese sulfate

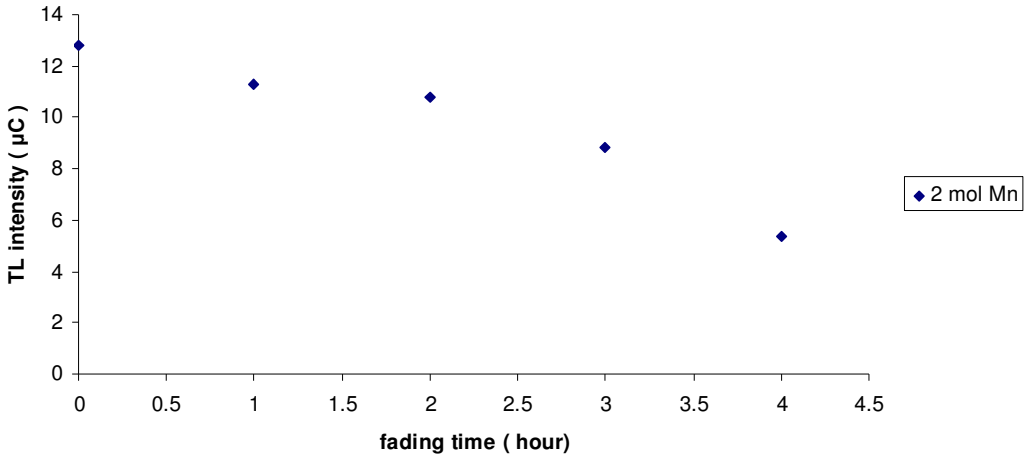

Figure 5.15 TL intensity vs fading time (hour) of ZnS nanophoshor doped with 2mol of manganese sulfate

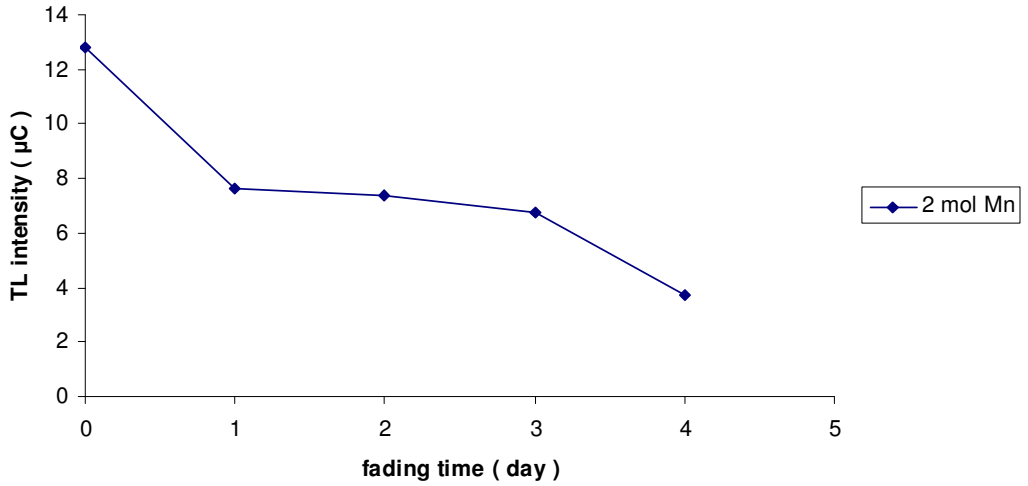

Figure 5.16 TL intensity vs fading time (day) of ZnS nanophoshor doped with 2mol of manganese sulfate

5.4.5. Fading of ZnS nanophoshor doped with 3mol of manganese sulfate

exposure time(sec)	dose rate(Gy/sec)	absorb dose(Gy)	fading	TL intensity (μC)
			No fading	9.1
			1 hour	7.2
			2 hour	6.8
			3 hour	5.7
591	0.091	53.8	4 hour	2.8
			1 day	7.2
			2 day	6.8
			3 day	5.7
			4 day	2.8

Table 5.12 exposure time, dose rate , absorb dose , fading and TL intensity of ZnS nanophoshor doped with 3mol of manganese sulfate

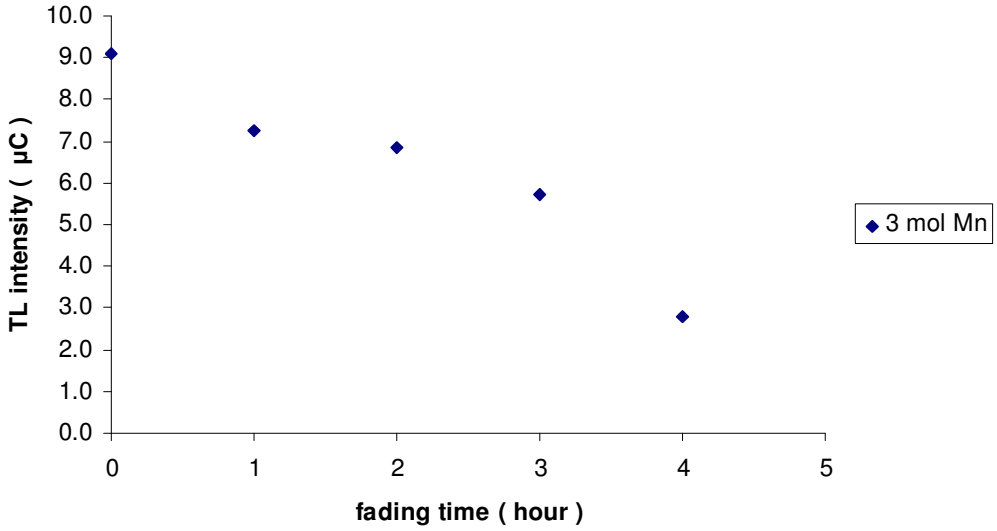

Figure 5.17 TL intensity vs fading time (hour) of ZnS nanophoshor doped with 3mol of manganese sulfate

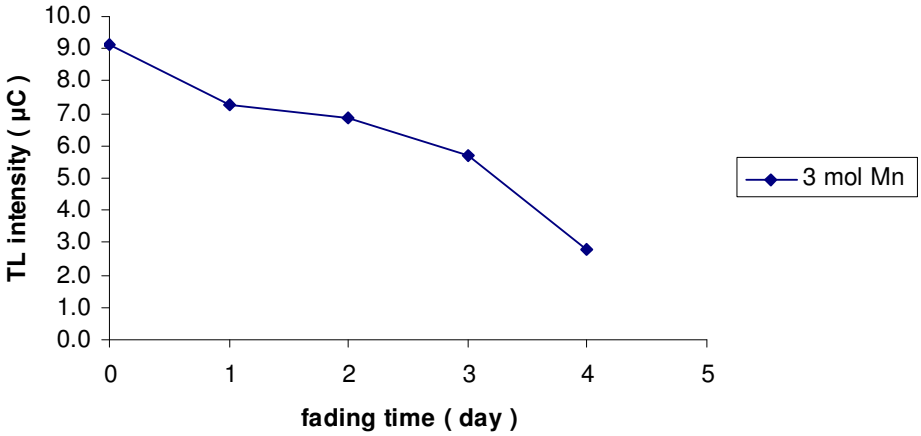

Figure 5.18 TL intensity vs fading time (day) of ZnS nanophoshor doped with 3mol of manganese sulfate

exposure time(sec)	dose rate(Gy/sec)	absorb dose(Gy)	fading	TL intensity (μC) 1 mol Mn	2 mol Mn	3 mol Mn	none Mn	TL intensity (nC) ZnS powder
591	0.091	53.8	No fading	12.9	12.8	9.1	6.2	9.4
			1 hour	11.3	11.3	7.2	4.7	9.1
			2 hour	10.6	10.8	6.8	4.2	7.9
			3 hour	8.2	8.9	5.7	3.7	8.3
			4 hour	5.2	5.3	2.8	3.1	7.1
			1 day	7.7	7.7	5.0	3.6	5.2
			2 day	7.6	7.4	5.2	2.8	5.1
			3 day	7.0	6.7	4.9	2.8	4.4
			4 day	3.5	3.7	1.9	2.2	3.9

Table 5.13 exposure time, dose rate , absorb dose , fading and TL intensity of ZnS doped with different Mn concentrations

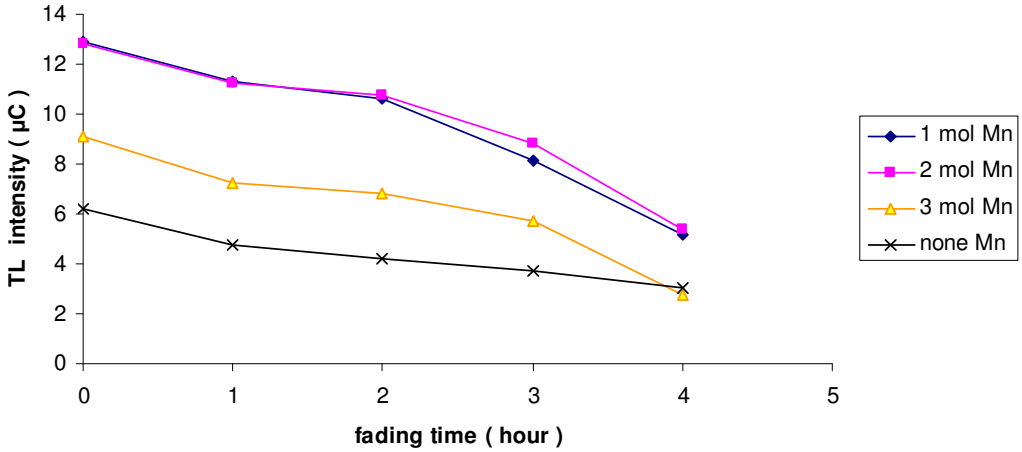

Figure 5.19 TL intensity vs fading time (hour) of ZnS nanophoshor doped with different Mn concentrations

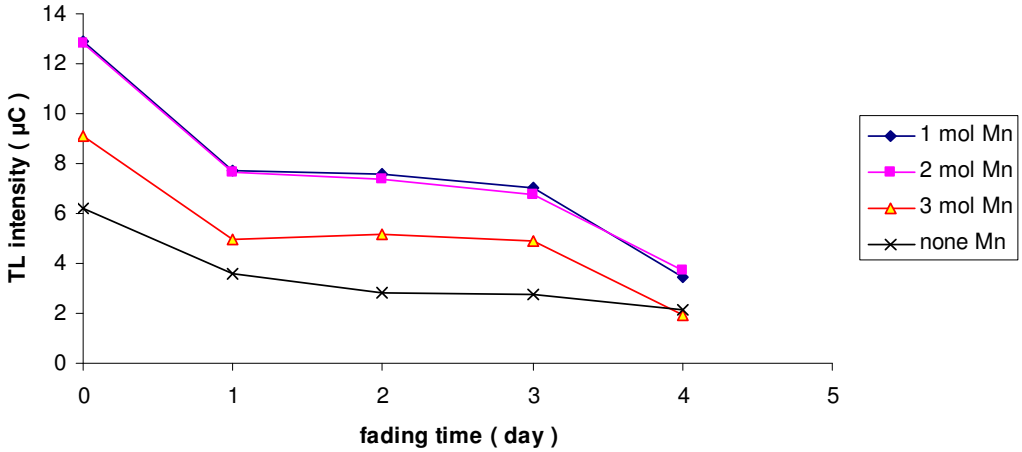

Figure 5.20 TL intensity vs fading time (day) of ZnS nanophoshor doped with different Mn concentrations

The thermal fading of glow peaks of ZnS:Mn were also measured for various durations at room temperature. FIGURE.6 shows the TL response of ZnS doped with different concentrations of Mn during four days. From the graph it can be seen that the ZnS doped with 1mole and 2 mole of Mn have low fading rate compared with the ZnS doped with 3 mole of Mn. For ZnS with 1mole and 2 mole of Mn the TL response loses approximately 40% of its original intensity after 1 day and this quantity is kept nearly constant for the next 2 days. After 4 days TL response loses 71% of its initial intensity.

5.5 ZnS nano particles synthesis by vapor transport deposition method

The silicon wafer covered with ZnS:Mn synthesis by vapor transport deposition method was Annealing and then exposed to a dose equal to 55 Gy, after that the thermoluminescence properties were studed by using Harshaw 3500 reader. The glow curve show a peak of 8nA intensity (fig 5.21)

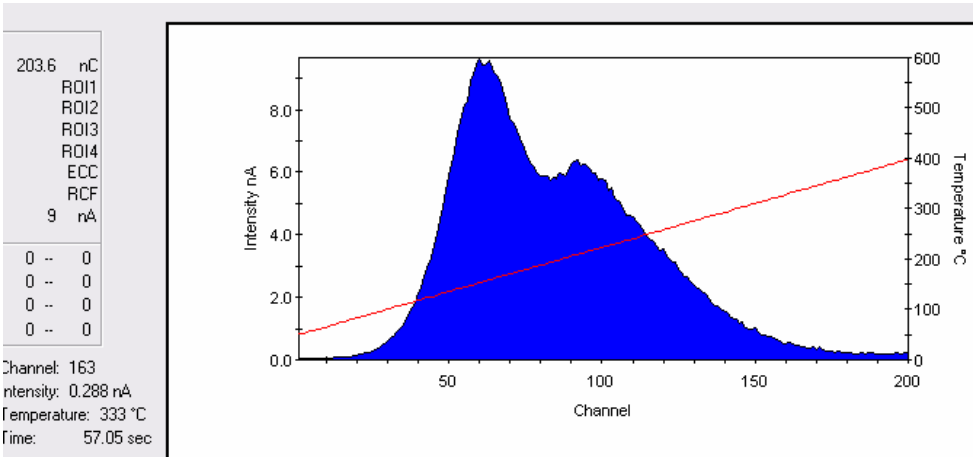

Figure 5.21 glow curve of ZnS:Mn nano particles made by vapor transport deposition method

30 mg of ZnS:Mn powder remains in the quartz tube was also Annealing and then exposed to a dose equal to 55 Gy and (fig 5.22) show the glow curve of this sample.

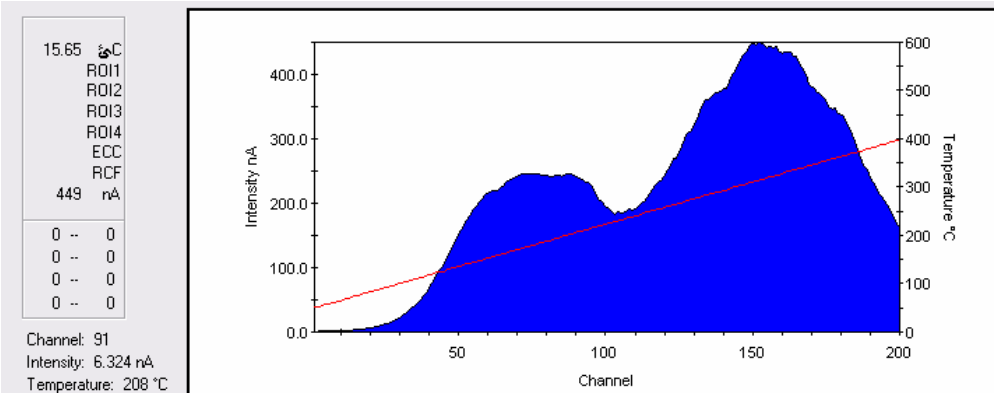

Figure 5.22 glow curve of ZnS:Mn powder remains in quartz tube

This powder gives a very high intensity equal to 400nA as it is shown in the previous figure.

The luminescence process in semiconductor nanoparticles is very complex phenomena and it was found that the luminescence of semiconductor nanoparticles is caused from the deep traps of surface states whose energy levels lie within the band gap of semiconductor. In nanophosphors, as the particle size is decreased the ions at the surface quickly increase. The excited electrons and holes from the surface ions are easily trapped at the surface states. So, by heating the sample the trapped carriers at the surface states are released and they recombine with each other and give out luminescence which is known as thermoluminescence. Decreasing the size of the particles makes the surface to volume ratio to be increased; which make the number of surface ions and surface states increase, so the number of trapped charged particles at surface state increases, as a result TL efficiency is increased. Therefore, the thermoluminescence enhancement of Mn-doped ZnS nanophosphor may be related with the surface states. [A. Necmeddin Yazici , 2007]

5.6 Zns nano particles as a thermoluminesence dosimeter.

Before the Zns nano particles are used as a thermoluminesence dosimeter, a calibration has to be done. There are many steps need to be followed to make the calibration. The first step is annealing. Then the element correction factor (Element Correction Coefficient, ECC) has to be measured with repetition process and linearity. After the previous methods are reached, calibration procedure will be done so that the ZnS powder can be used as a radiation dosimeter to detect the amount of absorbed dose after exposure.

The first step in the experiment is to selected 12 ZnS:Mn nano powder TLD (doped with 2mol of manganese sulfate). Those TLDs were divided into 4 groups, each group contains 3 TLD. Group (A_1, A_2, A_3), group (B_1, B_2, B_3), group (C_1, C_2, C_3), and group (D_1, D_2, D_3). The ZnS nano powders were put in small alumina containers. Each container contains 30 mg of ZnS nano powder.

5.6.1 Annealing process

The ZnS powder was annealed in the furnace at $500^{\circ}C$ and this temperature is reached with a constant heating rate then the samples are cooled gradually with constant rate to room temperature. After the annealing process is completed, the samples are stored in a black box to avoid any background radiation or any other source of light before they used as a radiation dosimeter.

Annealing process is very critical because it is used to return the dosimeters to their original condition especially when they had been irradiated at a very high dose. By annealing process the detection sensitivity of all used phosphors will be the same because the process will eliminate the thermal history for each dosimeter. The annealing process is very imported for the dosimeters that will be used for many time. After finished any TL reading, annealing process have to be done.

The second step in the experiment is annealing the four TLD groups by. The furnace which is used in this experiment is of model Vulcan 3-400HTA. The advantage of this furnace is the ability to be programmed to control the increasing and decreasing temperature in constant heating rate, also it can hold the required temperature for certain period of time. These properties are very important and critical in annealing process of TL dosimeters. The annealing cycle which has chosen is the one which consists of a high temperature anneal at $500^{\circ}C$ for 30 min followed by a low temperature anneal at $100^{\circ}C$ for 30 min. The furnace was programmed so that the samples were heated gradually to $500^{\circ}C$, $300^{\circ}C$ and $100^{\circ}C$. Each temperature was kept constant for 30 minute. The heating rate was equal to $40^{\circ}C/\min$.

5.6.2 Element Correction Coefficient, ECC

The TL efficiency is not exactly the same for all the TL dosimeters as a result of manufactured circumstances. To avoid this problem an Element Correction Coefficient, ECC is done. TL efficiency (TLE) is defined as emitted TL light intensity per unit of absorbed dose. All TL dosimeters do not give the same respond although they are constructed from the same material. Also, Element Correction Coefficient for all the dosimeters is used because they do not have similar masses correspond to each other.

After that the samples were exposed to a gamma ray by using Gamma cell 220 which use ^{60}Co as a source of gamma (γ) rays. The exposure time of the groups $(A_1, A_2, A_3), (B_1, B_2, B_3), (C_1, C_2, C_3)$ and (D_1, D_2, D_3) were 197sec, 395 sec , 592 sec and 789 sec respectively. Then the thermoluminescence properties were studied by using Harshaw 3500 reader (fig 5.23).